Aus der Klinik für Infektiologie und Mikrobiologie

der Universität zu Lübeck

Direktor: Prof. Dr. med. Jan Rupp

Der Einfluss von HIF-1α und metabolischen Interaktionen auf *Histoplasma capsulatum* Infektionen in Alveolarmakrophagen

Inauguraldissertation

zur

Erlangung der Doktorwürde

der Universität zu Lübeck

– Aus der Sektion Medizin –

vorgelegt von

Björn Lohse

aus Bremerhaven

Lübeck 2020

Erster Berichterstatter: Prof. Dr. med. Jan Rupp

Zweiter Berichterstatter: Prof. Dr. med. Christian Sadik

Tag der mündlichen Prüfung: 22.02.2021

zum Druck genehmigt. Lübeck, den 22.02.2021

Promotionskommission der Sektion Medizin

Table of Contents

List of figures

List of tables

Abbreviations

°C	degree Celsius
µL	microliter
µm	micrometer
2-DG	2-deoxy-glucose
A. dest.	distilled water
A. fumigatus	*Aspergillus fumigatus*
AM	alveolar macrophage(s)
APS	ammonium persulfate
ATP	adenosine triphosphate
BAL	bronchoalveolar lavage
BHI	brain-heart-infusion
BMDMΦ	bone marrow derived macrophage(s)
BSA	bovine serum albumin
CD	cluster of differentiation
CFSE	carboxyfluorescein N-hydroxysuccinimidyl ester
CFU	colony-forming unit
CO_2	carbon dioxide
DAPI	4’,6-diamidino-2-phenylindole
DC	dendritic cell(s)
(c)DNA	(complementary) deoxyribonucleic acid
DMOG	dimethyloxaloylglycine
DTT	1,4-dithiothreitol
ECAR	extracellular acidification rate
EDTA	ethylenediaminetetraacetic acid
EM	electron microscopy
EPO	erythropoietin
et al.	et alii
FACS	fluorescence-activated cell sorting
FCCP	carbonyl cyanide-p-trifluoromethoxyphenylhydrazone

$FeSo_4$	iron(II) sulfate
FIH	factor inhibiting HIF
g	gram
GLUT	glucose transporter
GM-CSF	granulocyte macrophage colony-stimulating factor
h	hour(s)
hpi	hours post infection
H. capsulatum	*Histoplasma capsulatum*
Hc	*Histoplasma capsulatum*
HEPES	4-(2-hydroxyethyl)-1-piperazineethanesulfonic acid
HIF	hypoxia inducible factor
hk	heat-killed
HMM	*Histoplasma*-macrophage medium
HOX	hypoxia
HRE	hypoxia responsive element
HRP	horseradish peroxidase
hsp60	heat-shock protein 60
IFN-γ	interferon gamma
Ig	immunoglobulin
IL	interleukin
IOX2	N-[[1,2-dihydro-4-hydroxy-2-oxo-1-(phenylmethyl)-3-quinolinyl]carbonyl]-glycine
KO	knock-out
L	liter
LPS	lipopolysaccharide
M	molar
M. tuberculosis	*Mycobacterium tuberculosis*
MDMΦ	monocyte-derived macrophage(s)
min	minute
mL	milliliter
MOI	multiplicity of infection

mTOR	mammalian target of rapamycin
MΦ	macrophage(s)
Na	sodium
NF-κB	nuclear factor kappa-light-chain-enhancer of activated B cells
nm	nanometer
O_2	oxygen
OCR	oxygen consumption rate
OXPHOS	oxidative phosphorylation
PAMP	pathogen-associated molecular pattern
PBS	phosphate-buffered saline
PCR	polymerase chain reaction
PDK	pyruvate dehydrogenase kinase
PenStrep	penicillin-streptomycin
PFA	paraformaldehyde
PHD	prolyl hydroxylase
pO_2	partial oxygen pressure
PRR	pathogen-recognition receptor
pVHL	von Hippel-Lindau tumor suppressor protein
qRT-PCR	quantitative real-time polymerase chain reaction
RBC	red blood cell
(m)RNA	(messenger) ribonucleic acid
ROS	reactive oxygen species
rpm	revolutions per minute
RT-PCR	reverse transcription polymerase chain reaction
SDS	sodium dodecyl sulfate
SDS-PAGE	sodium dodecyl sulfate polyacrylamide gel electrophoresis
SEM	standard error of the mean
Srb1	*Histoplasma capsulatum* sterol regulatory element binding protein

SREBP	sterol regulatory element binding protein
Syk	spleen tyrosine kinase
(T-)TBS	(Tween-)Tris-buffered saline
TEMED	N,N,N’,N’-Tetramethylethylenediamine
TNF-α	tumor necrosis factor alpha
V	volt
VLA	very-late antigen
WT	wild type

Abstract

Histoplasma capsulatum (*H. capsulatum*) is a dimorphic fungus and the causative agent of Histoplasmosis. While immunocompetent patients cope well with the infection, immunocompromised patients may experience severe or even fatal disease that includes the systemic spread of the fungus. Histoplasmosis is not contagious. Infection occurs from environmental reservoirs such as soil or bird droppings in endemic regions. These contain the infectious spores, which can be inhaled as aerosols. *H. capsulatum* performs a temperature dependent switch to the pathogenic yeast phase. Inside the lungs, it is phagocytized by resident alveolar macrophages (MΦ) but survives inside the MΦ. The interaction of host and pathogen leads to the creation of a survival niche. This includes the adaption to hypoxia due to granuloma formation, activation of metabolic pathways and inflammatory cytokine response. Herein, hypoxia-inducible factor 1α (HIF-1α) – a major regulator in mammalian cell metabolism and immune response during hypoxia and infection – was found to activate monocyte derived MΦ (MDMΦ) to degrade *H. capsulatum* without further activation of the adaptive immune system. This work elucidates the role of HIF-1α and metabolic changes with regard to pathogen survival for alveolar MΦ.

Alveolar MΦ stabilized HIF-1α during infection. Expression of the HIF-1α associated glycolytic target genes GLUT-1 and PDK1 was increased significantly. Also, the expression of pro-inflammatory genes IL-1β and TNF-α was found to be significantly upregulated. Investigating the survival of *H. capsulatum* in alveolar MΦ in a low oxygen environment (2% O_2, hypoxia) that resembles the *in vivo* situation in granuloma, a significant reduction in intracellular yeast numbers was found. In contrast, HIF-1α stabilizers could not activate alveolar MΦ to degrade *H. capsulatum*. Further, activation of immune cells depends on metabolic adaptations. Usually, this describes a switch from oxidative phosphorylation (OXPHOS) to glycolysis. In alveolar MΦ, both metabolic pathways were activated during infection. Analyzing the glycolytic activity in HIF-1α deficient alveolar MΦ, no difference was found compared to the wild type cells, indicating that glycolysis regulation is HIF-1α independent. Limiting glycolysis with 2-deoxy-glucose (2-DG) allowed alveolar MΦ to degrade *H. capsulatum*. This change was not due to lower phagocytosis or release of yeasts from dying MΦ, indicating *H. capsulatum* benefits from and even depends on the metabolic changes induced by the infection.

Conclusively, this work presents how *H. capsulatum* infection increases HIF-1α levels, promotes a metabolic activation and initiates an inflammatory response in alveolar MΦ. It shows that *H. capsulatum* needs sufficient O_2 supply for effective growth in alveolar MΦ. Finally, it reveals a novel mechanism for targeting *H. capsulatum* infection by glycolysis inhibition.

1. Introduction

1.1 Histoplasma capsulatum – the pathogen and its disease

Histoplasma capsulatum (H. capsulatum) was first described in the early 1900s by Samuel T. Darling. The name origins from its intracellular localization in macrophages (MΦ), also called histiocytes, and the false assumption that it is an encapsulated protozoan (plasmodium-like) pathogen (Darling 1906). In fact, *H. capsulatum* is a dimorphic fungus from the ascomycetes division. In the environment it grows as a mold in bird and bat guano enriched soil, forming infectious micro- and macroconidia that bud from the mycelia (Kasuga et al. 2003). Temperature is the main driver to induce the switch from mycelial to yeast phase. This switch is mandatory for *H. capsulatum* to express its virulent features (Medoff et al. 1986). Hence, the mycelia resemble the infectious and the yeasts the pathogenic phase.

The main areas of endemicity are along the Ohio and Mississippi river in the United States of America, where exposure rates are over 80% as determined by the histoplasmin skin test (Kauffman 2007; Antinori 2014). Cases in Europe are rare and usually the initial infection was acquired in the endemic areas, however there are rare cases of autochthonous infections in Italy and the UK (Ashbee et al. 2008).

Histoplasmosis – the disease caused by inhalation of *H. capsulatum* – is primarily a non-contagious pulmonary infection. Even though exposure to *H. capsulatum* is quite common, severe Histoplasmosis is rare. Infection usually manifests with flu-like symptoms in immunocompetent patients and will therefore be hardly ever diagnosed at this stage. However, suppression of the immune system may lead to severe cases, either as primary infection or reactivation of a dormant infection (Woods 2016). Reactivations of persistent infections have been shown to occur for as long as 50 years after the primary infection (Ashbee et al. 2008). In the era of therapy regimes with antibodies and check-point inhibitors for a large number of cancerous and autoimmune diseases along with the ever-growing life expectancies, opportunistic diseases – as severe Histoplasmosis in the majority of cases is – will come more into focus. Antimycotics like Amphotericin B or different Azoles provide effective therapeutic options in severe cases (Kauffman 2017). To keep an upper hand in the treatment options, a profound understanding of the biological mechanisms of infection is essential to reveal possible targets for pharmaceuticals.

1.2 Host-pathogen interaction

Upon inhalation, *H. capsulatum* spores reach the deeper airways, where their pathogen-associated molecular patterns (PAMPs) are recognized by pathogen-recognition receptors (PRRs) of phagocytes of the innate immune system. PRRs are a group of innate receptors on phagocytes that recognize specific PAMPs in the early response phase of infection and thereby orchestrate an innate immune response (Takeuchi and Akira 2010). Beta-(β-) Glucan, a polysaccharide PAMP commonly found in fungal cell walls, is recognized through Dectin-1, a C-type lectin PRR, causing a cytokine response by the host. Alpha-(α-) Glucan, however, physically shields β-Glucan, and is therefore a masking mechanisms of *H. capsulatum* to evade this recognition (Guimarães et al. 2011). To phagocytize *H. capsulatum* yeasts, MΦ recognize the heat shock protein 60 (hsp60) on the fungal surface by their CD11/CD18 receptor (Long et al. 2003). Interestingly, dendritic cells (DCs) bind and phagocytize *H. capsulatum* yeasts by their fibronectin receptor very-late antigen-5 (VLA-5), giving an approach to their ability to consequently degrade *H. capsulatum* for antigen presentation (Gildea et al. 2001). In contrast, MΦ are unable to kill and degrade *H. capsulatum* without activation of the innate immune system (Newman et al. 1992). In this context, pro-inflammatory cytokines like interleukin (IL)-12, interferon gamma (IFN-γ), tumor necrosis factor alpha (TNF-α) and granulocyte macrophage colony-stimulating factor (GM-CSF) have been shown to play a crucial role in activating murine MΦ followed by fungal clearance (Wu-Hsieh et al. 1992; Zhou et al. 1995; Deepe et al. 1999; Vignesh et al. 2013). However, mechanisms eliciting MΦ's antifungal activity are distinct between murine and human models. Apart from the above-mentioned cytokines, also M-CSF and IL-3 mount protection in human MΦ, whereas the role of IFN-γ is under debate (Deepe 2000). Besides that, human MΦ do not rely on phagosomal acidification, but show a respiratory burst upon infection as opposed to murine MΦ (Horwath et al. 2016).

As MΦ are unable to kill *H. capsulatum* directly, their infection induces the formation of granuloma in various organs like the spleen, liver and lungs. Granuloma can form due to delayed-type hypersensitivity and non-degradable agents at inflammation sites. MΦ as such, in the form of epithelioid cells or multinucleated giant cells are the predominating cell type along with $CD4^+$ T helper cells. Central caseation necrosis is another typical phenomenon (Kobayashi et al. 2001). In their immunological function granuloma are a double-edged sword. On the one hand, they contain the pathogen, prevent dissemination and protect the healthy surrounding tissue. On the other hand, *H. capsulatum* is able to overcome environmental stress factors like limited nutrient supply, acidification and especially hypoxia caused by the microenvironment in granuloma and therefore finds a niche to evade eradication (Heninger et al. 2006). It has been shown that granuloma as such and

especially the MΦ inside are hypoxic, making the adaptive mechanisms of the pathogen and host a decisive determinant for the outcome of infection (DuBois et al. 2016).

Deducting from this, *in vitro* experiments, that were based on an infection model with monocyte derived MΦ (MDMΦ), showed that hypoxia – through the stabilization of the hypoxia-inducible factor (HIF) 1α – provides an environment for MDMΦ to elicit fungicidal activity against *H. capsulatum* (Friedrich 2016). In those MDMΦ HIF-1α levels are enhanced by *H. capsulatum* infection. Despite the fact that HIF-1α is usually described as an inducer of the metabolic shift towards an enhanced glycolysis (Cheng et al. 2014), both of the main pathways for cellular energy supply oxidative phosphorylation (OXPHOS) and glycolysis showed higher turnovers. Creating an environment of excess HIF-1α by chemical protein stabilization with dimethyloxaloglycine (DMOG) enhanced the expression of glycolytic genes and pro-inflammatory cytokines during infection but decreased functional glycolytic activity. This created a microenvironment in which the formerly susceptible MDMΦ were able to degrade *H. capsulatum* even under normoxic conditions. Summarizing the findings, HIF-1α shapes the host response to *H. capsulatum* infection in MDMΦ by increasing the expression of pro-inflammatory cytokines and glycolytic genes and altering metabolic activity. Even though MDMΦ provide a good model, the primary infection site harbors mainly alveolar MΦ, which will be the focus of this thesis. Hence, a closer differentiation of the different MΦ populations is necessary.

1.3 Tissue specific macrophages – a distinct population

Generally, MΦ are part of the myeloid lineage and resemble one of the phagocyte populations of the innate immune system. Their main task is to degrade cellular debris or foreign material and orchestrate an inflammatory response. Monocytes and their precursors are harbored in the bone marrow and patrol the blood as an ever-ready intervention force to infiltrate an inflammation focus, where they differentiate to MΦ. Therefore, they resemble the recruited MΦ (Varol et al. 2015). Nevertheless, MΦ are not only on-call, but also permanently situated in the tissue, examples being Langerhans-cells in the skin or Kupffer cells in the liver. In the lungs, alveolar MΦ are the resident tissue specific MΦ population. They fulfil specific tasks in their niche, such as the clearance of surfactant protein and are also the first-line of defense as they are already present at the site of interest (Davies et al. 2013). As for all tissue specific MΦ, alveolar MΦ are a self-renewing cell population originating from the prenatal structures yolk sac and fetal liver (Yona et al. 2013). They are long-lived cells that show a characteristic pattern of surface markers, making them a distinct population. *In vivo* they are tightly controlled by the lung epithelium via cell-cell and paracrine mechanisms to prevent a hyperinflammatory response caused by the constant exposure to environmental agents (Hussell and Bell 2014). To further distinguish them from recruited MΦ, alveolar MΦ metabolism predominantly relies on OXPHOS. Even though the lungs provide sufficient supply of O_2 to do so in healthy situations, hypoxic environments

in the lungs are not unusual. In this case, alveolar MΦ show greater potential to adapt by switching to anaerobic glycolysis than other MΦ types (Simon et al. 1977; Fels and Cohn 1986).

Alveolar MΦ also fulfil their task as first line of defense in Histoplasmosis. It has been shown that their phagocytic potential against *H. capsulatum* is comparable to MDMΦ, but with different patterns of recognition receptors (Newman et al. 1990). In mouse models, their fungicidal capacity was described similar to other MΦ types (Brummer and Stevens 1995). This is important to lay ground for experiments with alveolar MΦ, since in scientific approaches the experimental set-up usually uses MΦ differentiated from precursor cells, such as the bone marrow derived MΦ (BMDMΦ) in murine or the MDMΦ in human models. These MΦ are easily accessible in large quantities but compared to the *in vivo* situation they most closely resemble the population of recruited MΦ. To study the initial and early phase of a *H. capsulatum* infection, experiments with alveolar MΦ provide a more suitable approach. Assessing how alveolar MΦ interact with *H. capsulatum,* and how they handle the challenges at the infection site is crucial for understanding the course of infection.

1.4 Hypoxia in the context of infection and inflammation

Higher energy demands, thrombosis, necrosis and compression create a hypoxic environment at inflammatory sites, meaning a lower O_2 concentration at the focus compared to the surrounding (Eltzschig and Carmeliet 2011). However, the definition of hypoxia and normoxia always depends on the context. While *in vivo* definition varies, as also tissues and organs vary in their physiological oxygenation (Carreau et al. 2011), hypoxia *in vitro* is defined as 1 - 3 % partial O_2 pressure and normoxia as the partial atmospheric O_2 pressure at sea level of 20.9 % (Nizet and Johnson 2009). The effect of hypoxia on infection outcomes has been investigated as early as the 1950s, where it was found that mice kept under lower oxygen conditions showed decreased bacterial burdens after *Mycobacterium tuberculosis (M. tuberculosis)* infection (Sever and Youmans 1957). Indeed, later studies showed that a hypoxic environment leads to enhanced phagocytic and antimicrobial capacity in myeloid cells (Schaible et al. 2010). In general, hypoxia forces cells to adapt, as the usual energy acquirement through oxidative phosphorylation (OXPHOS) relies on O_2 and is therefore insufficient under hypoxia. Alternatively, energy can be generated through glycolysis, which is oxygen independent (Fangradt et al. 2012).

Looking at the pathogen's side, the ability to adapt to hypoxia is a vital feature, since not only inflammatory sites but also their environmental niches like the soil can be hypoxic (Maček et al. 2011). In fungal pathogens like *H. capsulatum,* but also in *Cryptococcus neoformans* and *Aspergillus fumigatus (A. fumigatus)*, virulence and growth are attenuated under hypoxic conditions (Grahl et al. 2012). Fungi mainly sense oxygen availability via the sterol synthesis, a highly O_2 consumptive process (Rosenfeld

and Beauvoit 2003). In *H. capsulatum* – as in many other fungi – a homologue of the human sterol regulatory element binding protein (SREBP) called Srb1 is found. Srb1 as a transcription factor induces genes known to be involved in the transport of metabolites, sterol biosynthesis and coping with nitrosative stress. Also, it has been linked directly to growth and virulence (DuBois and Smulian 2016). In the end, the interplay of pathogen and host-cell adaptation shapes the outcome of infection.

1.5 HIF-1α in mammalian cells

The hypoxia-inducible factor (HIF) was first discovered as an inducer of the erythropoietin (EPO) gene expression under hypoxic conditions (Semenza et al. 1991). Today it is known to be a major regulator in the cellular adaptation to the lower oxygen availability at hypoxic sites, but also to regulate metabolism and inflammation under normoxic conditions. To become active as a transcription factor, the α-subunit needs translocate to the nucleus where it forms a heterodimer with the constitutively present β-subunit which binds to the hypoxia-response elements (HREs). There are three isoforms of HIFα: HIF-1α, HIF-2α and HIF-3α of which HIF-1α is the most thoroughly investigated one (Lee et al. 2004). Typical transcriptional targets of HIF-1α are metabolic and angiogenic genes, allowing cell homeostasis under hypoxic conditions (Weidemann and Johnson 2008; Iyer et al. 1998).

Under normoxic conditions, HIF-1α – being cytosolically located – is hydroxylated by the oxygen-dependent prolyl-hydroxylases (PHDs) which leads to the recognition and ubiquitylation by the von Hippel-Lindau tumor suppressor protein (pVHL) and subsequent proteasomal degradation of HIF-1α. Another regulator of HIF-1α degradation is factor inhibiting HIF (FIH). FIH hydroxylates HIF-1α and thereby prevents its binding to a co-activator (p300-CREB) which is necessary to bind HIF-1α to the DNA. Under hypoxic conditions, HIF-1α cannot be hydroxylated and protein levels rise so that nuclear translocation, dimerization and gene transcription can be initiated. In addition to the oxygen dependent ones, various other regulation mechanisms have been described that do not rely on hypoxia. Nuclear factor kappa-light-chain-enhancer of activated B cells (NF-κB) seems to be a potent inducer of HIF-1α transcription and is therefore required for HIF-1α protein accumulation. Furthermore, IL-1β and lipopolysaccharide (LPS) are examples of HIF-1α inducers even under normoxia (Bhandari and Nizet 2014).

Besides its function as a physiological regulator of cell homeostasis, HIF-1α plays an important role in pathological conditions such as cardiovascular, pulmonary or oncological diseases, but also in immunity and infectious diseases (Semenza 2000). In the latter, different bacterial infection models – either by HIF-1α knock-outs or pharmacological stabilization of HIF-1α - have shown beneficial effects of HIF-1α on the infection outcome (Schaffer and Taylor 2015). In different fungal infections, there are implications that HIF-1α accumulates due to protein stabilization and transcriptional regulation and is

required to contain infection. Herein, mice deficient in myeloid HIF-1α succumbed to infection with *H. capsulatum* and *A. fumigatus* (Friedrich et al. 2017). It has therefore been discussed as a potential therapeutic target in multiple clinical settings (Bhandari and Nizet 2014).

Increasing HIF-1α levels in experimental settings is commonly done by using chemical inhibitors of PHDs to prevent the degradation of the abundant HIF-1α protein. Some authors call these chemical inhibitors "hypoxia mimetics" (Cartee et al. 2012). Whether or not this term reflects their function appropriately is under debate. Generally, these PHD inhibitors allow a more precise investigation of the changes caused by HIF-1α, whereas numerous variables change when actual hypoxic conditions are applied. Because confounding factors of the hypoxic environment are absent when using chemical PHD inhibitors, experimental results can be more specifically attributed to the elevated HIF-1α levels (Ahmed 2018). Since the overall aim of research targeting HIF-1α in infectious models is the establishment of a therapeutic intervention *in vivo,* a substance-based approach rather than a condition-based approach is desired. Within the group of PHD inhibitors two commonly used substances are DMOG and IOX2. Even though DMOG inhibits multiple PHDs, it is a well-established and frequently used chemical in experimental settings. Hence, results obtained can be well compared to and matched with other studies when using DMOG (Berra et al. 2003, Friedrich 2016). In contrast, IOX2 very specifically inhibits the subtype 2 of PHDs. HIF-1α is mostly hydroxylated by PHD2 rather than other PHDs. Therefore, IOX2 allows a very specific modulation of HIF-1α levels (Chowdhury et al. 2013). Nonetheless, studies using IOX2 are rarer compared to those using DMOG. Some even argue that DMOG should be preferably used, if the experimental aim is to chemically mimic hypoxia and not only investigate HIF-1α (Chan et al. 2016).

1.6 Immunometabolism

In mammalian cells glucose is metabolized in the cytosol through glycolysis to provide pyruvate for OXPHOS inside the mitochondria to supply energy in the form of adenosine triphosphate (ATP). This provides the maximum ATP production per molecule of glucose (Heiden et al. 2009). However, mammalian cells and especially immune cells show different degrees of activation and proliferation, and have to function under varying conditions concerning O_2 and substrate availability. Therefore, they require adaptive mechanisms for their metabolism (Mosser and Edwards 2008).

The Warburg effect describes the switch from OXPHOS to glycolysis in tumor cells despite normoxic conditions. Glycolysis under these conditions is therefore termed aerobic glycolysis, which may equip cells with an evolutionary advantage to face hypoxia (Gatenby and Gillies 2004). Upon activation of resting MΦ, a metabolic switch similar to the Warburg effect is described (Kelly and O'Neill 2015). Herein, pro-inflammatory MΦ – also termed M1 – exhibit a glycolytic phenotype and utilize

mitochondria to generate reactive oxygen species (ROS), whereas alternatively activated MΦ – also termed M2 – show an enhanced OXPHOS (Pearce and Pearce 2013).

For intracellular pathogens the activation of glycolysis has been directly linked to the MΦ's killing capacity. In most cases, increased glycolysis resulted in a more effective pathogen clearance (Wyatt et al. 2016; Gleeson et al. 2016). However, Czyz *et al.* found that in the case of *Brucella abortus* infection the pathogen exploits the host cells' enhanced glycolysis to optimize its own replication. For the first time, they mention inhibitors of glycolysis as a possible treatment option for infectious diseases (Czyz et al. 2017).

The regulatory function of HIF-1α in immunometabolism is described as a driver of the switch towards a glycolytic phenotype, including the upregulation of glycolytic genes such as the glucose transporter GLUT-1 or PDK1 (Covarrubias et al. 2015). HIF-α $^{-/-}$ myeloid knockout cells show reduced ATP levels and consequently reduced cell motility and killing capacity in a model of BMDMΦ and group B streptococcus (Cramer et al. 2003). Herein, murine cell models provide the advantage of having established mouse breeds with a HIF-1α knockout in the myeloid cell lineage. This allows determining whether changes in the cellular metabolism during infections are signaled via HIF-1α.

1.7 Objective

In recruited MΦ, the role of HIF-1α as a regulator of metabolism, inflammation and pathogen control has been described. As an intracellular pathogen, the interaction of *H. capsulatum* with the host cell and exploitation of its resources is crucial. Herein, the host cell metabolism is of particular importance. In the course of *H. capsulatum* infection, alveolar MΦ are the first phagocytes to recognize the pathogen.

To evaluate how *H. capsulatum* evades its control and clearance, understanding the primary response at the site of infection is utterly important. The goal of this thesis is to gain a better understanding of the "first line of defense" by elucidating the role of hypoxia and its marker protein HIF-1α in resident alveolar MΦ during *H. capsulatum* infection. Special attention will be paid to metabolic adaptation of the host cell.

The aims of this study are:

1.) To analyze stabilization levels of HIF-1α during infection and hypoxia.
2.) To describe the changes of known downstream HIF-1α targets, such as inflammatory and metabolic genes as well as functional cell metabolism and its interaction with HIF-1α.
3.) To assess the survival of intracellular yeasts under hypoxia, chemical HIF-1α stabilization and inhibition of glycolysis.

2. Materials and Methods

2.1 Materials

2.1.1 Machines and devices

Table 1: Machines and devices

Centrifuges	Centrifuge 5810 R	Eppendorf, Hamburg, Germany
	Legend Micro 21R	Thermo Fisher Scientific, Waltham, MA, USA
	Centrifuge 5417R	Eppendorf, Hamburg, Germany
	Heraeus Pico	Thermo Fisher Scientific, Waltham, MA, USA
	4-15C	Sigma-Aldrich, St. Louis, MO, USA
	Multifuge 3 S-R	Thermo Fisher Scientific, Waltham, MA, USA
Hoods	SterilGARD Hood	The Baker company, Sanford, ME, USA
	SterilGARD III	The Baker company, Sanford, ME, USA
	SterilGARD II	The Baker company, Sanford, ME, USA
	Clean Air Spie	Colandis, Kahla, Germany
	Biohit Antares 48 Biohazard	Biohit, Finland
	2-410 H Abzug	Köttermann, Uetzen-Hänigsen, Germany
	PCR workstation	Peqlab Life-Science, Erlangen, Germany
Incubators	Napco 6300 (37°C, 5% CO_2)	Marshall Scientific, Hampton, NH, USA
	CO_2 Incubator 610 (37°C, 5% CO_2)	Fisher Scientific Company LCC, Pittsburg, PA, USA
	Imperial II Incubator (29°C, 0% CO_2)	Lab Line Instruments, Dubuque, Iowa, USA
	Hypoxia incubator chamber with single flow meter	STEMCELL Technologies, Köln, Germany
	Thermo Forma Series II Water Jacketed	Fisher Scientific Company LCC, Pittsburg, PA, USA
	DP-80 Cryo porter	Arctiko, Esbjerg, Denmark
	Midi 40	Fisher Scientific Company LCC, Pittsburg, PA, USA

Stirrers, Shakers, Vortex	Vortex Genie 2	Fisher Scientific Company LCC, Pittsburg, PA, USA
	Reax 2000	Heidolph, Schwabach, Germany
	Stirrer	Curtin Matheson Scientific, Houston, TX, USA
	DS-500 orbital shaker	VWR, Radnor, PA, USA
	Rocker Platform	Bellco Biotechnology, Vineland, NJ, USA
	Universal shaker SM 30 A with an incubation hood TH15	Edmund Bühler GmbH, Hechingen, Germany
	KS 260 basic	IKA, Staufen, Germany
Scales, pH meter	XS-210	Denver Instrument, Bohemia, NY, USA
	KB 600-2	Kern&Söhne, Balingen, Germany
	AT261 Delta Range	Mettler-Toledo, Columbus, OH, USA
	Accumet Basic AB15	Fisher Scientific Company LCC, Pittsburg, PA, USA
	MP220	Mettler-Toledo, Columbus, OH, USA
Microscopes	Telaval 31	Carl-Zeiss, Oberkochen, Germany
	Mircomaster	Fisher Scientific Company LCC, Pittsburg, PA, USA
	Colony Counter	American Optical Corporation, Dashfield, Quebec, CAN
	Axiovert-25	Carl-Zeiss, Oberkochen, Germany
	BZ-9000E	Keyence, Osaka, Japan
Water baths	Innova 3000	New Brunswick Scientific, Edison, NJ, USA
	P/S Thelco Model 83	Precision Scientific Co., India
	Water bath	Memmert GmbH, Büchenbach, Germany

PCR systems, Imagers

GeneAmp PCR System 9700	Applied Biosystems, Foster City, CA, USA
7500 Fast Real-Time PCR System	Applied Biosystems, Foster City, CA, USA
Light Cycler 480II	Roche, Basel, Switzerland
C1000 Thermal Cycler	BioRad, Hercules, CA, USA
FluorChem HD2	Cell Biosciences, Palo Alto, CA, USA
Fusion Fx 7	Vilber Lourmat, Eberhardzell, Germany

Western blot devices

Mini Gel Tank	Life Technologies, Carlsbad, CA, USA
Mini Trans Blot Cell	Bio-Rad Laboratories, Hercules, CA, USA
Model 250	Bethesda Research Laboratories, NJ, USA
Power PAC 3000	Bio-Rad Laboratories, Hercules, CA, USA

Pipets, pipet tips

P10, P20, P200, P1000	Gilson, Inc, Middleton, WI, USA
Eppendorf reference (10 µL, 100µL, 1000µL)	Eppendorf, Hamburg, Germany
Pipet-aid	Drummunod Scientific Co., Broomall, PA, USA
Accu Jet Pro	Brand GmbH, Wertheim, Germany
Serological pipettes (5mL, 10mL, 25mL)	TPP, Trasadingen, Switzerland
Pipette tips	Fisher Scientific Company LLC, Pittsburgh, PA, USA
Biosphere Filter Tips	Sarstedt AG & Co, Nümbrecht, Deutschladn

2.1.2 Buffers

Table 2: Buffers

Name	Composition
Blocking buffer	5 g skim milk powder, 100 ml T-TBS buffer
5X Electrophoresis buffer	15 g Tris, 72 g glycine, 5 g SDS, ad 1 L A. dest.
FACS buffer	5 g BSA, 50 mg NaN_3, 5 mL human serum, ad 500 mL PBS
Lysis buffer	3.94 g Tris HCl, 40 ml glycerol, 8 g SDS, 20 mL DTT (1 M), bromophenol blue, ad 200 mL A. dest., pH 7.8
Monti fixative	156 mL 0.12 M sodium cacodylate, 25 mL 25 % glutaraldehyde, 19 mL 10 % PFA, 3 ml 3 % NaCl, ad 100 mL A. dest., pH 7.35
PBS	80 g NaCl, 2 g KCl, 11.5 g NaH_2PO_4 x $12H_2O$, 2 g KH_2PO_4, ad 1 L A. dest., pH 7.2
Red blood cell lysis (RBC) buffer	8.26 g NH_4Cl, 1,0 g $KHCO_3$, 0.037 g EDTA ad 1 L A. dest.
Separation gel buffer	90.5 g Tris, ad 500 mL A. dest., pH 8.8
Stacking gel buffer	30 g Tris, ad 500 mL A. dest., pH 6.8
10X TBS	24.2 g Tris, 80 g NaCl, ad 1 L A. dest., pH 7.6
T-TBS	100 ml TBS buffer (10x), 1 mL Tween-20, ad 1 L A. dest.
Transfer buffer	3 g Tris, 14.4 g glycine, 200 mL methanol, ad 1 L A. dest.

2.1.3 qRT-PCR primers and reagents

Primers for murine experiments were purchased as indicated below.

Table 3: Murine qRT-PCR primers

Primer	Supplier
β-Actin (Mm02619580)	Applied Biosystems, Foster City, CA, USA
GLUT-1 (Mm00441480)	Applied Biosystems, Foster City, CA, USA
HIF-1α (Mm00468869)	Applied Biosystems, Foster City, CA, USA
IL-1β (Mm00434228)	Applied Biosystems, Foster City, CA, USA
PDK1 (Mm00554300)	Applied Biosystems, Foster City, CA, USA
TNF-α (Mm00443258)	Applied Biosystems, Foster City, CA, USA

Primers for human experiments were purchased from TIB MOLBIO (Berlin, Germany) with below indicated sequences. According to the data sheet, RNase-free H_2O was used for dilution to a final concentration of 20 µM.

Table 4: Human qRT-PCR primer sequences

Primer	Sequence
β-Actin	Forward CCT GGC ACC CAG CAC AAT Reverse GGG CCG GAC TCG TCA TAC
HIF-1α	Forward GGC AGC AAC GAC ACA GAA ACT GA Reverse TGA TCC TGA ATC TGG GGC ATG GT
GLUT1	Forward GGT TGT GCC ATA CTC ATG ACC Reverse CAG ATA GGA CAT CCA GGG TAG C
PDK1	Forward GGT TGG GAA CCA CTC TTT CA Reverse GAT GGC TCT GAT GCT TTG GT
IL-1β	Forward TCC CCA GCC CTT TTG TTG A Reverse TTA GAA CCA AAT GTG GCC GTG
TNF-α	Forward CCC AGG GAC CTC TCT CTA ATC Reverse ATG GGC TAC AGG CTT GTC ACT

Table 5: PCR reagents

PCR reagents	Supplier
Random primer	Roche, Basel, Switzerland
Dinucleotide mix	Roche, Basel, Switzerland
Maxima reverse transcriptase	Thermo Fisher Scientific, Waltham, MA, USA
Ribolock	Thermo Fisher Scientific, Waltham, MA, USA
RT buffer	Thermo Fisher Scientific, Waltham, MA, USA
SYBR GREEN I Master Mix	Roche, Basel, Switzerland
TaqMan Universal PCR Master Mix	Applied Biosystems, Foster City, CA, USA
Reverse Transcription System	Promega, Madison, WI, USA

2.1.4 Western blot antibodies

Table 6: Antibodies for western blot

Antibody	Dilution	Supplier
Anti-β-Actin (rabbit)	1:500	Santa Cruz Biotechnology Inc., Santa Cruz, CA, USA
Anti-β-Actin (rabbit)	1:2000	Cell Signaling Technology, Danvers, MA, USA
Anti-HIF-1α (rabbit)	1:1000	Abcam, Cambridge, MA, USA
Anti-HIF-1α (mouse)	1:500	BD Bioscience, Heidelberg, Germany
Anti-rabbit, HRP conjugate (goat)	1:5000	Invitrogen, Rockford, IL, USA
Anti-mouse IgG, HRP-conjugate (horse)	1:2000	Cell Signaling Technology, Danvers, MA, USA
Anti-rabbit IgG, HRP-conjugate (goat)	1:4000	Cell Signaling Technology, Danvers, MA, USA

2.1.5 Immunofluorescence reagents

Table 7: Immunofluorescence reagents

Reagent	Dilution/ Concentration	Supplier
Anti-HIF-1α (rabbit)	1:1000	Abcam, Cambridge, MA, USA
Anti-rabbit, Alexa Fluor 594 conjugate (goat)	1:1000	Cell Signaling Technology, Danvers, MA, USA
Carboxyfluorescein N-hydroxysuccinimidyl ester (CFSE)	10 µM	Thermo Fisher Scientific, Waltham, MA, USA
4',6-diamidin-2-phenylindol (DAPI)	1:2000	Sigma-Aldrich, St. Louis, MO, USA

2.1.6 Cell culture media

Table 8: Cell culture media

Medium	Composition
Human alveolar macrophage culture	500 mL RPMI 1640, 20 mL human serum, 5 mL PenStrep, 5 mL HEPES, 5 mL L-Glutamine, 1 mL β-mercaptoethanol (0.064%)
Murine alveolar macrophage culture	500 mL RPMI 1640, 10% Fetal bovine serum, 500 µL Gentamicin, 1 mL β-Mercaptoethanol (0.064%)
Glyco Stress Test	RPMI 1640 (R1383), 1 mM Na-Pyruvate
Mito Stress Test	RPMI 1640 (R6504), 1 mM Na-Pyruvate
Liquid *H. capsulatum* culture	10,6 g Ham's F-12, 18,2 g Glucose/Dextrose, 1,0 g glutamic acid, 10,0 mL cystine (0.84 g Cystine in 50 mL 1N HCl), 6,0 g HEPES ad 1,0 L A. dest.

2.1.7 Agar

Table 9: Agar

Agar	Composition
Mycosel agar	18 g Mycosel agar, 4 g Bacto agar, 5 g glucose, 0.05 g cystine, 250 µL Gentamicin ad 500 mL A. dest. + 250 mL sheep blood
Histoplasma macrophage medium (HMM) agar	2x agarose (8 g agarose, ad 500 mL H_2O) + 2x HMM (10.6 g Ham's F12, 1 g glutamic acid, 18.2 g glucose, 5.96 g HEPES, 10 mL PenStrep, 5 mL $FeSO_4$, 10 mL Cystine, 1.5 mL Genatmicin, ad 500 mL A. dest., pH 7.5)
Brain heart infusion (BHI) agar slants	26 g BHI ad 500 mL A. dest.

2.1.8 Consumables

Table 10: Consumables

Blotting paper	Schleicher & Schuell, Dassel, Germany
Cell culture plate, 48, 24 well	Greiner Bio-One GmbH, Frickenhausen, Germany
Cell culture plate, 96 well ½ area	Corning Inc., Corning, NY, USA
Cell culture plate, 96 well	TPP, Trasadingen, Switzerland
Cell culture plate, 96 well black	Thermo Fisher Scientific, Waltham, MA, USA
Conical Tubes (50 mL, 15 mL)	Thermo Fisher Scientific, Waltham, MA, USA Sarstedt AG &Co, Nümbrecht, Germany
Coverslips glass 10 mm	Menzel GmbH, Braunschweig, Germany
Coverslips plastic 13mm	Thermo Fisher Scientific, Waltham, MA, USA
Cryotubes	Nalge Nunc, Rochester, NY, USA
Erlenmeyer flask	Bellco Biotechnology, Vineland, NJ, USA
Glass plates mini protean	Bio-Rad Laboratories, Hercules, CA, USA
Hemocytometer	Reichert, Buffalo, NY, USA
Neubauer chamber	Hassa Laborbedarf, Lübeck, Germany
NucleoSpin RNA kit	Machery-Nagel, Düren, Germany
Inoculation loop (10 µL)	Greiner Bio-One GmbH, Frickenhausen, Germany
Needle (18G, 20G)	Becton Dickinson and Company, Franklin Lakes, NJ, USA
Nitrocellulose membrane (0.2 µm)	Bio-Rad Laboratories, Hercules, CA, USA
Nitrocellulose membrane	GE Healthcare, Little Chalfont, Great Britain
Novex WedgeWell, 4-20% Tris- Glycine- Gel (10 well, 15 well)	Thermo Fisher Scientific, Waltham, MA, USA
Parafilm	Carl Roth GmbH, Karlsruhe, Germany

PCR MicroAmp Fast Optical 96 well plate	Applied Biosystems, Foster City, CA, USA
PCR multiwell plate 96	Roche, Basel, Switzerland
Petri dishes	Thermo Fisher Scientific, Waltham, MA, USA
Pipette tips	Fisher Scientific Company LLC, Pittsburgh, PA, USA
Round-Bottom Tube (5 mL)	Corning Inc., Corning, NY, USA
Reaction tubes (2 mL, 1.5 mL, 0.5 mL)	Sarstedt AG &Co, Nürnbrecht, Germany
Syringes (1 mL, 10 mL, 30 mL)	Becton Dickinson and Company, Franklin Lakes, NJ, USA
Tissue culture flask (150 mL)	TPP, Trasadingen, Switzerland
Transfer pipette	Fisher Scientific Company LLC, Pittsburg, PA, USA
Tubing Adapter, 20G	Becton Dickinson and Company, Franklin Lakes, NJ, USA
Vacutainer CPT	Becton Dickinson and Company, Franklin Lakes, NJ, USA

2.1.9 Chemicals

Table 11: Chemicals

Acrylamide (40%)	Bio-Rad Laboratories, Hercules, CA, USA
Agarose Seakem ME	Lonza Group AG, Basel, Switzerland
Ammonium Chloride	Fisher Scientific Company LLC, Pittsburg, PA, USA
Ammonium persulfate (APS)	Sigma-Aldrich, St. Louis, MO, USA
Antimycin A	Sigma-Aldrich, St. Louis, MO, USA
Bacto Agar	Becton Dickinson and Company, Franklin Lakes, NJ, USA
Bambanker cryopreservation	Wako Chemicals GmbH, Neuss, Germany
BHI Agar	Becton Dickinson and Company, Franklin Lakes, NJ, USA
Bromphenol blue	Serva Electrophoresis GmbH, Heidelberg Germany
Bovine serum albumin (BSA)	Sigma-Aldrich, St. Louis, MO, USA
L-Cystine	Fisher Scientific Company LLC, Pittsburg, PA, USA Sigma-Aldrich, St. Louis, MO, USA
2-Deoxy-Glucose (2-DG)	Sigma-Aldrich, St. Louis, MO, USA
Dextrose	Fisher Scientific Company LLC, Pittsburg, PA, USA
Dimethyl sulfoxide	Sigma-Aldrich, St. Louis, MO, USA
Dimethyloxaloylglycine (DMOG)	Cayman Chemicals, Ann Arbor, MI, USA
1,4-dithiothreitol (DTT)	Roche, Basel, Switzerland
Ethanol	Merck KGaA, Darmstadt, Germany
Ethylenediamine Tetraacetic Acid (EDTA)	Sigma-Aldrich, St. Louis, MO, USA
Carbonyl cyanide-p-trifluoromethoxyphenylhydrazone (FCCP)	Cayman Chemicals, Ann Arbor, MI, USA
Fetal Bovine Serum HyClone	Thermo Fisher Scientific, Waltham, MA, USA
$FeSO_4$	Merck KGaA, Darmstadt, Germany
Gentamicin Sulfate	Sigma-Aldrich, St. Louis, MO, USA
Gentamicin Sulfate	MP Bio, Santa Ana, CA, USA
Glycine	Fisher Scientific Company LLC, Pittsburg, PA, USA
L-Glutamic Acid	Fisher Scientific Company LLC, Pittsburg, PA, USA
L-Glutamic Acid	Honeywell, Morris Plains, NJ, USA
L-Glutamine	Lonza Group AG, Basel, Switzerland
Glycerol	Merck KGaA, Darmstadt, Germany
Glycine	AppliChem GmbH, Darmstadt, Germany
Ham`s F12 powder	Sigma-Aldrich, St. Louis, MO, USA
Ham`s F12 liquid medium	Life Technologies, Carlsbad, CA, USA
HEPES powder	Sigma-Aldrich, St. Louis, MO, USA
HEPES solution	Pan-Biotech GmbH, Aidenbach, Germany
Hypoxia gas mix (2% O_2, 5% CO_2, 93% NO)	Air Liquid, Düsseldorf, Germany
IOX2	Cayman Chemicals, Ann Arbor, MI, USA
Lipopolysaccharide (LPS)	Sigma-Aldrich, St. Louis, MO, USA

2-Mercaptoethanol	Sigma-Aldrich, St. Louis, MO, USA
Methanol	Merck KGaA, Darmstadt, Germany
Mycosel Agar	Becton Dickinson and Company, Franklin Lakes, NJ, USA
NaCl	Fisher Scientific Company LLC, Pittsburg, PA, USA
NaN_3	Sigma-Aldrich, St. Louis, MO, USA
Non-fat dry milk	Kroger, Cincinnati, OH, USA
Oligomycin A	Cayman Chemicals, Ann Arbor, MI, USA
Paraformaldehyde (PFA)	Sigma-Aldrich, St. Louis, MO, USA
Penicilline-Streptomycine	Sigma-Aldrich, St. Louis, MO, USA
Phosphate-Buffered Saline (PBS)	Corning Inc., Corning, NY, USA
Potassium Bicarbonate	Fisher Scientific Company LLC, Pittsburg, PA, USA
Presto Blue Reagent	Invitrogen, Frederick, MD, USA
Rotenone	Cayman Chemicals, Ann Arbor, MI, USA
RPMI 1640 HyClone	GE Healthcare, Little Chalfont, Great Britain
RPMI 1640 Gibco	Life Technologies, Carlsbad, CA, USA
Soap 7X	MP Bio, Santa Ana, CA, USA
sodium dodecyl sulfate (SDS)	Merck KGaA, Darmstadt, Germany
Seahorse XF^e96 FluxPack	Agilent, Santa Clara, CA, USA
Sheep Blood, defibrinated	Colorado Serum Company, Denver, CO, USA
Skim milk powder	Sigma-Aldrich, St. Louis, MO, USA
Sodium Pyruvate	MP Bio, Santa Ana, CA, USA
Spectra Multicolor Broad Range Protein Ladder	Thermo Fisher Scientific, Waltham, MA, USA
SuperSignal West Femto	Thermo Fisher Scientific, Waltham, MA, USA
N,N,N',N'-Tetramethylethylenediamine (TEMED)	Sigma-Aldrich, St. Louis, MO, USA
Tris Base	Fisher Scientific Company LLC, Pittsburg, PA, USA Merck KGaA, Darmstadt, Germany
TritonX	Sigma-Aldrich, St. Louis, MO, USA
Trypan Blue	Sigma-Aldrich, St. Louis, MO, USA
Tween 20	Fisher Scientific Company LLC, Pittsburg, PA, USA

2.1.10 Mice

Murine cells were harvested from male C57BL/6 mice, which were ordered from The Jackson Laboratory (Bar Harbor, ME, USA). With the help of Dr. Timothy Eubank (Ohio State University, OH, USA) a Lyz2cre HIF-1α fl/fl (HIF-1$\alpha^{-/-}$) strain was established. Microisolator cages for mice were located at the Department of Laboratory Animal Medicine (University of Cincinnati, Cincinnati, OH, USA), which is accredited by the Association for Assessment and Accreditation of Laboratory Animal Care (AAALAC, Frederick, MD, USA). Experiments were conducted according to the Animal Welfare Act Guidelines of the National Institutes of Health (NIH, Bethesda, MD, USA) and protocols approved by the Institutional Animal Care and Use Committee of the University of Cincinnati (Cincinnati, OH, USA).

2.2 Methods

2.2.1 Primary cell culture

2.2.1.1 Human alveolar macrophages

Alveolar MΦ were obtained from patients undergoing bronchoalveolar lavage (BAL) for diagnostic reasons at the Medical Department III of the University Clinic of Schleswig-Holstein, Campus Lübeck. Trained physicians performed the procedure of BAL. In short, patients were sedated with midazolam and 2% lidocaine was used for local anesthesia before the bronchoscopically guided lavage was performed by instillation and immediate reaspiraton of 0.9% NaCl. Recovery volume was noted for each patient. BAL samples were stored at 4°C until their further processing. All procedures were performed according to German national guidelines and approved by the ethics committee of the University of Lübeck on August 4th, 2016 (file reference 16-198).

To remove mucus clumps, BAL samples were passed through a four layered gauze, collected in 50 mL tubes and centrifuged at 170*g for 10 minutes (min). Contamination with red blood cells was lysed by incubation in 0.1 % NaCl for 1 min. Cells were resuspended in RPMI 1640 Medium and stored at 4°C until their further processing. Here cells were pelleted at 170*g for 10 min and washed in 50 mL PBS to remove lose material. Subsequently, cells were resuspended in medium and the alveolar MΦ were counted as described in chapter 2.2.2. Cells were seeded into tissue culture plates at a concentration of 5*10^5 in 1 mL human alveolar MΦ culture medium for 48-well cell culture plates and 1*10^5 in 200 µL for 96-well cell culture plates. Cells were allowed to adhere at 37 °C, 5% CO_2 for 90 min. Non-adherent cells were removed and fresh medium was added to the wells. After overnight incubation (37 °C, 5% CO_2) medium was changed before experiments started. The chemical additives DMOG (100 µM), IOX2 (50 µM) and 2-DG (1 mM, 5 mM) were used at concentrations commonly described in publications addressing HIF-1α in MΦ (Deppe et al. 2015, Acosta-Iborra et al. 2009, Tannahil et al. 2013, Friedrich 2016).

2.2.1.2 Murine alveolar macrophages

To obtain murine alveolar MΦ, mice were euthanized by application of CO_2 for 10 min and cervical dislocation. Mice were stretched out and sprayed down with 70% ethanol. A small incision was made on the ventral side and mice were skinned. The trachea was surgically exposed using forceps and scissors. To deflate the lungs and improve the cell yield per mouse, the diaphragm was carefully dissected, and a piece of the rib cage cut out to provide space for the lungs to inflate after instillation. A wooden stick was laid underneath the trachea to stabilize it. The trachea was punctured with an 18G needle, a blunted 20G tubing adapter was then carefully inserted and fixed with suture. Using a 1 mL syringe, 1 mL PBS was instilled into the lungs and reaspirated. Using the same volume, the lungs were flushed up to ten times. Cells were collected on ice. Cells from two to seven mice were pooled per experiment.

Cell containing collection tubes were filled with PBS and cells were centrifuged at 1600 rpm for 10 min. The supernatant was discarded. RBC lysis was performed on ice for 5 min using 2 mL RBC lysis buffer. Tubes were filled to 50 mL with PBS to dilute the lysis buffer. Tubes were spun at 1600 rpm for 10 min. Supernatant was then fully discarded and cells were resuspended in 250 µL murine alveolar MΦ medium. Cells were then counted as explained in chapter 2.2.2 and seeded into 96-well half area plates at a density of 7.5* 10^4 in a working volume of 100 µL and adhered overnight. The plates were kept at 37°C, 5% CO_2 overnight.

2.2.2 Cell counts

Cells were diluted 1:5 with trypan blue and 10 µL of this dilution were loaded onto a hemacytometer. Alveolar MΦ were identified by size and shape, differential cell counts from the department of pulmonology were used as a guideline. Trypan blue identified dead cells, which were excluded from the count. One of the four corner squares (consisting of 4x4 smaller squares) was counted and the cell number per volume was calculated as follows:

$$cells/mL = \frac{cells\ counted\ x\ dilution\ factor\ x\ 10^4}{number\ of\ squares\ counted}$$

2.2.3 Hypoxia experiments

For those experiments carried out under hypoxic conditions, culture plates were placed into a portable hypoxia chamber. To prevent evaporation of medium, an open H_2O filled petri dish was also put in the chamber. To purge the chamber, a constant flow of 20 L/min was applied for 3 min with the help of a single flow meter from a portable gas bottle, containing pre-mixed gas (2% O_2, 5% CO_2, 93% N_2)

2.2.4 Fungal culture and host cell infection

2.2.4.1 H. capsulatum culture

H. capsulatum was grown on BHI agar slants. Slants were made by mixing 26 g BHI with 500 mL distilled water (A. dest.) and autoclaving it for 15 min at 121 °C. Test tubes were positioned at a 20° angle and filled with 8 mL liquid agar. Agar slants were allowed to solidify for 4 h and then stored at 4 °C. *H. capsulatum* from the strain G217B was obtained from American Type Cell Culture Collection (ATCC, Manassas, VA, USA) and grown on BHI slants at 37 °C and 5% CO_2. *H. capsulatum* were passed onto a new slant weekly.

2.2.4.2 Liquid H. capsulatum culture

For infection experiments, *H. capsulatum* was grown in liquid culture for two to four days to grow yeasts to mid-log phase. For that purpose, yeasts were flushed off agar slants and cultured in 50 mL of Ham's F12 medium in a shaking flask at 37 °C. To harvest *H. capsulatum*, liquid culture was spun at 2000 rpm for 5 min, supernatant was discarded, and pelleted yeasts were resuspended in 20 mL PBS. To separate clumps from single yeasts, the suspension was spun again at 300 rpm for 5 min. The top half of the centrifuged suspension – representing the single yeast fraction – was transferred to another tube and vortexed to split up possibly remaining yeast clumps. To count *H. capsulatum* yeasts for infection, a 1:40 dilution in PBS was prepared from the single cell suspension and loaded onto a hemocytometer. When counting, every two yeasts with direct connection – meaning they are budding from one another – were counted as one (e.g. 1 bud = 1 count, 2 buds = 1 count, 3 buds = 2 counts and 5 buds = 3 counts). For calculation, the formula from chapter 2.2.2 was applied.

If not elsewise indicated, infection experiments were performed with five yeasts per MΦ (MOI (multiplicity of infection) = 5:1).

2.2.4.3 H. capsulatum stock conservation

To prepare *H. capsulatum* stocks, yeasts were taken off the agar slants with inoculation loops and transferred to cryotubes with 1 mL Bambanker cryopreservation medium and stored at -80 ˚C.

2.2.4.4 Recovering and plating H. capsulatum

To quantify the intracellular number of yeasts, viable *H. capsulatum* was recovered from alveolar MΦ to be plated. After 24 h, supernatant was removed (and saved for plating) from the culture wells and alveolar MΦ were lysed with 200 µL A. dest for 5 min. Successful lysis was checked under the light microscope. The lysate was mixed by pipetting up and down and transferred to a conical tube filled with 4.5 mL PBS. Wells were washed with 300 µL PBS that were also transferred to the conical tube. A series of 1:10 dilutions was prepared by mixing 100 µL of the previous dilution with 900 µL PBS. Dilutions usually went down to 10^{-3} (dilution number = 3). Each dilution was thoroughly vortexed. Agar

plates were virtually split in half and 50 µL of a respective dilution were spread on each side of the plate with single-use spreaders. Agar plates were stacked, placed in plastic bags and incubated for 7 days (HMM plates at 37 °C, 5 % CO_2 and Mycosel plates at 29 °C, room air) before counting colonies. Total colony forming units were calculated by the formula below and expressed as percentage of the control.

$$total\ CFUs = \frac{colonies\ on\ whole\ plate}{2}\ x\ 10^{2}\ x\ 10^{-\ (dilution\ number)}$$

2.2.5 Molecular-biological methods

2.2.5.1 Western blot

The supernatants were removed by pipetting. Adherent cells were lysed using 100 µL western blot lysis buffer and then manually detached by thoroughly scraping the well bottom with a pipet tip. The cell lysates were transferred to 1.5 mL reaction tubes and stored at -25°C until their analysis. Separation of proteins by their molecular weight was done using sodium dodecyl sulfate polyacrylamide gel electrophoresis (SDS-PAGE) (Laemmli 1970). Gels were either casted by hand or purchased as pre-casted 10 or 15 pocket gels. For the hand casted gels (Table 12), the bottom phase resembling the 10% separation gel was casted first and overlaid with A. dest. during 25 min of polymerization. After decanting the A. dest., 4% stacking gel was added and a 10- or 15-pocket comb inserted. After 15 min of polymerization combs were removed and gels were placed into electrophoresis chambers. Electrophoresis chambers were filled, and gel pockets washed with electrophoresis buffer.

Table 12: Electrophoresis gel composition

Reagent	Volume (mL) in 4% stacking gel	Volume (mL) in 10% separation gel
A. dest.	1.6	2.45
Tris (0.5 M)	0.625	
Tris (1.5 M)		1.25
Acrylamide	0.25	1.25
10 % SDS	0.025	0.05
TEMED	0.0025	0.0025
10 % APS	0.125	0.025

To denaturate proteins, cell lysates were heated at 95 °C for 5 min. Samples were mixed and the gel pockets were loaded with 25 µL cell lysate per sample. One pocket was filled with 5 µL broad range marker to reproduce the size of the separated proteins. All empty pockets were filled with 25 µL lysis buffer.

A voltage of 70 V was applied for 15 min to move proteins through the stacking gel, followed by 55 min with a constant voltage of 200 V to separate proteins in the separation gel.

Subsequently, proteins were blotted from the gel onto a nitrocellulose membrane. Therefore, the gel and membrane were laid against each other between two filter papers and sponge mats in a clamping device and loaded into cooled blotting chambers filled with cold blot buffer. A voltage of 75 V was applied for 90 min.

The membrane was cut according to the broad range marker to separate HIF-1α and β-Actin. The membrane was blocked for 1 h at room temperature with 5% skim milk on a shaker. Membranes were incubated with 10 mL primary antibody diluted in skim milk overnight at 4 °C on a shaker. The next day, membranes were washed with 15 mL T-TBS for 15 min twice and then incubated with the horseradish peroxidase linked secondary antibody diluted in skim milk for 60 min.

Using the oxidation of luminol and the principle of enhanced chemiluminescence, protein bands were visualized in an imager. Densitometry was performed using Bio1D software. The intensity of investigated protein bands was normalized to the 0 hours post infection (hpi) sample and its respective β-Actin intensity.

2.2.5.2 RNA extraction

To extract the RNA from cells, the supernatant was removed from the cell culture wells and the adherent cells were lysed using 350 µL RA1 lysis buffer supplemented with 3.5 µL β-mercaptoethanol for cells in 48-well plates. Half the volume was used in 96-well plates. After the lysis, the well bottom was scraped with a pipet tip, and the cell lysate was transferred to a 1.5 mL reaction tube. Samples were stored at -80 °C until they were analyzed.

RNA was extracted from the cell lysates using an RNA extraction kit, following the user's manual instructions. In short, lysates were filtered to reduce viscosity, and RNA was then bound to a membrane. DNA was digested, the membrane was desalted and washed to elute the RNA in 40 µL of RNase-free H_2O eventually. Part of the extracted RNA was submitted to reverse transcriptase- PCR (RT-PCR) and the remaining RNA stored at -80 °C.

2.2.5.3 Reverse transcriptase polymerase chain reaction

RT-PCR was used to generate complementary DNA (cDNA) from extracted messenger RNA (mRNA) transcripts. Table 13 shows the reagents used for one reverse transcriptase-PCR reaction.

Table 13: RT-PCR master mix composition

Reagent	Volume (µL)
RNase-free H_2O	5.5
5X Reaction Buffer	4
Dinucleotide Mix	2
Random primer	2
RevertAid transcriptase	1
RiboLok RNase Inhibitor	0.5
mRNA sample	5

The reaction was run in a thermal cycler following the heating and cooling periods listed in Table 14. cDNA was stored at -20°C until it was used for quantitative real time (qRT)-PCR reaction.

Table 14: RT-PCR reaction steps

Program step	Temperature	Duration
Hybridization	25 °C	10 min
Reverse Transcription	50 °C	30 min
Enzyme Inactivation	85 °C	5 min
Holding	4 °C	Forever

2.2.5.4 Quantitative real time-PCR

To quantify and compare the mRNA levels of different samples, the produced cDNA was submitted to qRT-PCR. Reagents for the reaction were prepared according to Table 15. The reactions were run in a 96-well plate cycler system and SYBR-Green or TaqMan detection was used to determine DNA amplification. A total of 45 cycles was determined as the endpoint of the experiment. Each cycle consisted of the heating and cooling steps listed in Table 16. To display results as fold changes, crossing points of target genes were analyzed by the ΔΔCt method. β-Actin was used as the housekeeping gene for normalization.

Table 15: qRT-PCR reagents

Reagent	Volume (µL)
2X master mix	10
cDNA	2
Primer (forward and reverse)	0.2 each
H_2O	7.6

Table 16: qRT-PCR reaction steps

Light Cycler 480 (SYBR-Green based)

Procedure	Temperature	Duration
Denaturation	95°C	10 min
Program	95°C	10s
(45 cycles)	60°C	5s
	72°C	10s
Melting curve	95°C	1s
	50°C	30s
Cooling	40°C	15s

7500 Fast Real-Time PCR System (TaqMan based)

Procedure	Temperature	Duration
Holding	50 °C	20 s
Denaturation	95 °C	10 min
Program	95 °C	15 s
(40 cycles)	60 °C	1 min

2.2.6 Metabolic analysis of alveolar macrophages

2.2.6.1 Mito stress test

To analyze the mitochondrial respiration of murine alveolar MΦ, the Seahorse XF Mito Stress Test was performed using the Seahorse XFe 96 analyzer. For that purpose, murine alveolar MΦ were seeded into Seahorse XF 96-well cell culture plates at a density of $5*10^4$ per well in a volume of 80 µL. Cells were then rested under the sterile hood for one hour to allow even cell distribution and were then kept at 37 °C and 5% CO_2 overnight until the experiment was started. The sensor cartridge was loaded with 200 µL Seahorse XF Calibrant one day before the experiment and was kept at 37 °C without CO_2. *H. capsulatum* was prepared for infection as described in chapter 2.2.4.2. The Mito Stress Test medium was adjusted to pH 7.4 ± 0.1. 6 hpi the cell culture medium was replaced by washing the wells twice with the Mito Stress Test medium. 20 µL were left in the wells between washing steps. The final well volume was adjusted to 175 µL. After the washing, cells were rested for at least 1 h at 37 °C without CO_2. The injection ports of the sensor cartridge were loaded with a constant volume of 25 µL per port. The final working concentrations for each component are shown in Table 17. The protocol run on the Seahorse XFe 96 Analyzer is shown in Table 18.

Table 17: Port loading scheme for Mito Stress Test

Port	Compound	Concentration [µM]	Effect
A	Oligomycin	1.0	Inhibition of ATP synthase
B	FCCP	0.7	Uncoupling the electron transport chain
C	Rotenone/Antimycin A	1.0	Inhibition of complex I and III

Table 18: Protocol for Seahorse runs

Pre-Run	Basal	First injection	Second injection	Third injection
No injection *Calibration* *Equilibration* *(12 min)*	No injection 3 cycles: Mix (3 min) Measure (3 min)	Injection Port A 3 cycles: Mix (3 min) Measure (3 min)	Injection Port B 3 cycles: Mix (3 min) Measure (3 min)	Injection Port C 3 cycles: Mix (3 min) Measure (3 min)

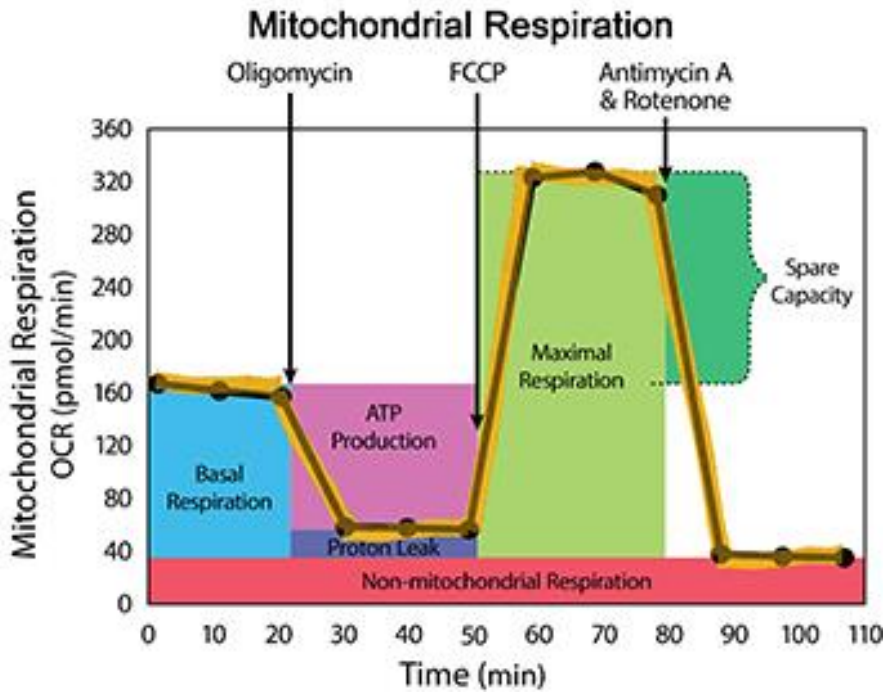

Figure 1: Profile of mitochondrial respiration during Mito Stress Test (agilent.com)

Calculation of the parameters “Basal respiration”, “ATP Production” and “Maximal respiration” is explained in Figure 1 and was performed accordingly.

2.2.6.2 Analysis of glycolysis

To analyze the glycolytic activity of murine alveolar MΦ, the Seahorse XF Glycolysis Stress Test was performed using the Seahorse XFe 96 analyzer. For that purpose, the murine alveolar MΦ cell culture, sensor cartridge and infection were prepared and handled as described for the Mito Stress Test. The Glycolysis Stress Test medium was pH adjusted to 7.35 ± 0.05. 6 hpi the cell culture medium was replaced by washing the wells twice with the Glyco Stress Test medium. The final working concentrations for each component loaded into the sensor cartridge are shown in Table 19. The protocol run is shown in Table 18.

Table 19: Port loading scheme for Glyco Stress Test

Port	Compound	Concentration	Effect
A	Glucose	10 mM	Substrate of glycolysis
B	Oligomycin	1.0 µM	Inhibition of ATP-synthase
C	2- deoxy-D-glucose	100 mM	Inhibition of glycolysis

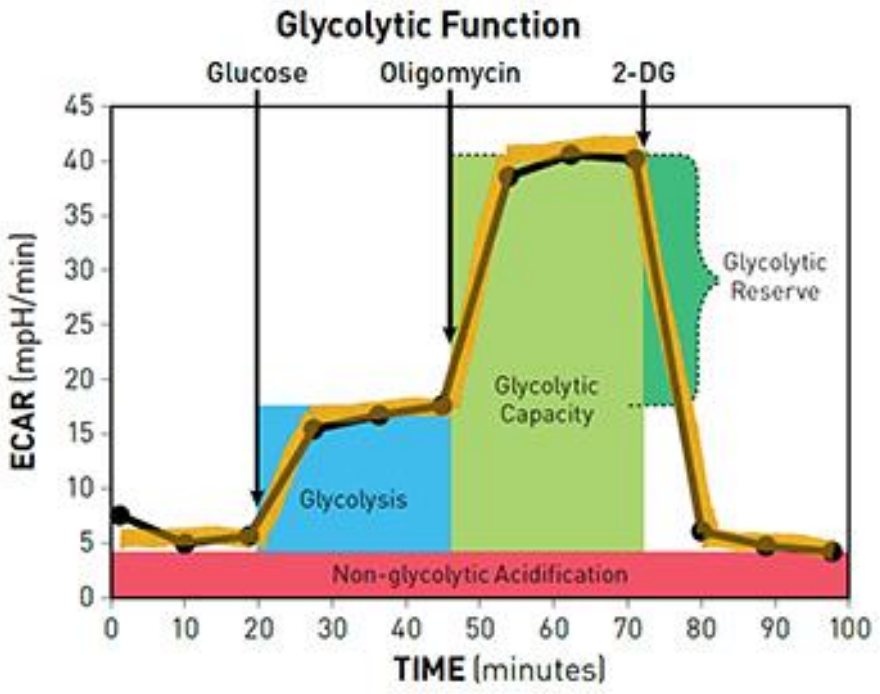

Figure 2: Profile of glycolytic function during Glycolysis Stress Test (agilent.com)

Calculation of the parameters "Glycolysis", "Glycolytic Capacity" and "Non-glycolytic Acidification" is explained in Figure 2 and was performed accordingly.

2.2.7 Immunofluorescence

2.2.7.1 CFSE labeling

Carboxyfluorescein N-hydroxysuccinimidyl ester (CFSE), a live-cell fluorescence dye, was used to visualize intracellular *H. capsulatum*. *H. capsulatum* yeasts were stained with 10 µM CFSE in PBS at 37 °C and 5% CO_2. After 15 min the staining process was quenched with a fivefold volume of human alveolar MΦ medium. Yeasts were then counted for infection according to chapter 2.2.2. All working and incubation steps including CFSE were carried out protected from the light to prevent the dye from fading.

2.2.7.2 Imaging HIF-1α

For immunofluorescence experiments, $3*10^5$ human alveolar MΦ were seeded into 48-well cell culture plates with glass cover slips placed in each well. The infection experiment was carried out with a MOI 5:1 of CFSE-labeled *H. capsulatum*. 6 hpi the experiment was terminated by removing the medium and fixing the cells in 3% paraformaldehyde (PFA) for 30 min. Cells were washed in 10 µM glycine in PBS three times to remove PFA and stored in PBS at 4 °C overnight. To allow intracellular staining, cells were permeabilized with 0.1% Triton X in PBS for 5 min and washed with PBS three times afterwards. To reduce unspecific binding of antibodies, cells were blocked with FACS buffer for 30 min. For primary antibody incubation, a wet chamber was prepared to reduce evaporation. A soaked paper towel was laid into a plastic box and covered with a piece of parafilm. A 20 µL drop of primary antibody at the prepared dilution was given onto the parafilm. Coverslips were removed from the culture plates with forceps. The cell-covered side was placed onto the antibody solution on parafilm and incubated for 1 h. Coverslips were returned to the cell culture plate, washed with PBS three times and covered with secondary antibody at the prepared dilution for 30 min at 37 °C and 5% CO_2. Secondary antibody was removed with three washes in PBS. Nuclei were stained with DAPI (4',6-diamidin-2-phenylindol) for 15 min. DAPI was removed by two PBS washes and one wash with A. dest. Cover slips were placed onto microscope slides with mounting fluid and stored at 4 °C overnight. A Keyence BZ-9000E fluorescence microscope was used and images were taken with the 100x oil immersion lens. All working and incubation steps including CFSE labeled *H. capsulatum* or fluorescent secondary antibody were carried out protected from the light, to prevent fading.

2.2.8 Electron microscopy

Human alveolar MΦ infected with *H. capsulatum* for 24 h were fixed with Monti fixative for 1 h and stored at 4 °C. 1% OsO_4 in 0.1 M cacodylate buffer was used for a 2 h post-fixation step. Following dehydration with graded ethanol series, samples were embedded in araldite (Fluka, Buchs, Switzerland). The ultra-thin cut, uranyl acetate and lead citrate stained sections were imaged in a JEOL JEM 1011 transmission electron microscope (TEM).

2.2.9 Statistical analysis

Data from single experiments was assembled in charts using Microsoft's Excel 2010. To test for significances, collected data was transferred to GraphPad's Prism 7. Data sets comprised of more than two conditions were tested with one-way ANOVA (Turkey's or Sidak's multiple comparison test). In cases where only two conditions were compared, Student's t-test was performed. Significances were defined as *p<0.05, **p<0.01 and ***p<0.001. Data is presented as mean ± SEM (standard error of the mean).

3. Results

3.1 The role of HIF-1α in *H. capsulatum* infected alveolar macrophages

3.1.1 Influence of *H. capsulatum* on HIF-1α

HIF-1α is a regulator for the maintenance of cell homeostasis under hypoxic conditions. Not only hypoxia but also various pathogens – bacterial and fungal – are known to influence HIF-1α levels under normoxic conditions. Hence, the influence of *H. capsulatum* on HIF-1α in alveolar MΦ was investigated. Alveolar MΦ were infected with *H. capsulatum* for 6 hours (h). To differentiate between an active modulation by the viable pathogen and a solely receptor mediated effect, cells were also exposed to heat-killed yeasts for protein analysis. Based on the results gained, following experiments were mostly carried out with viable *H. capsulatum*. Samples were analyzed by western blot for protein quantity. Since elevation of protein levels can be due to either protein stabilization – a well described post-transcriptional mechanism in *H. capsulatum* infection – or enhanced expression of the *hif1a* gene, HIF-1α mRNA amount was determined by qRT-PCR for the 6 hpi time point, too.

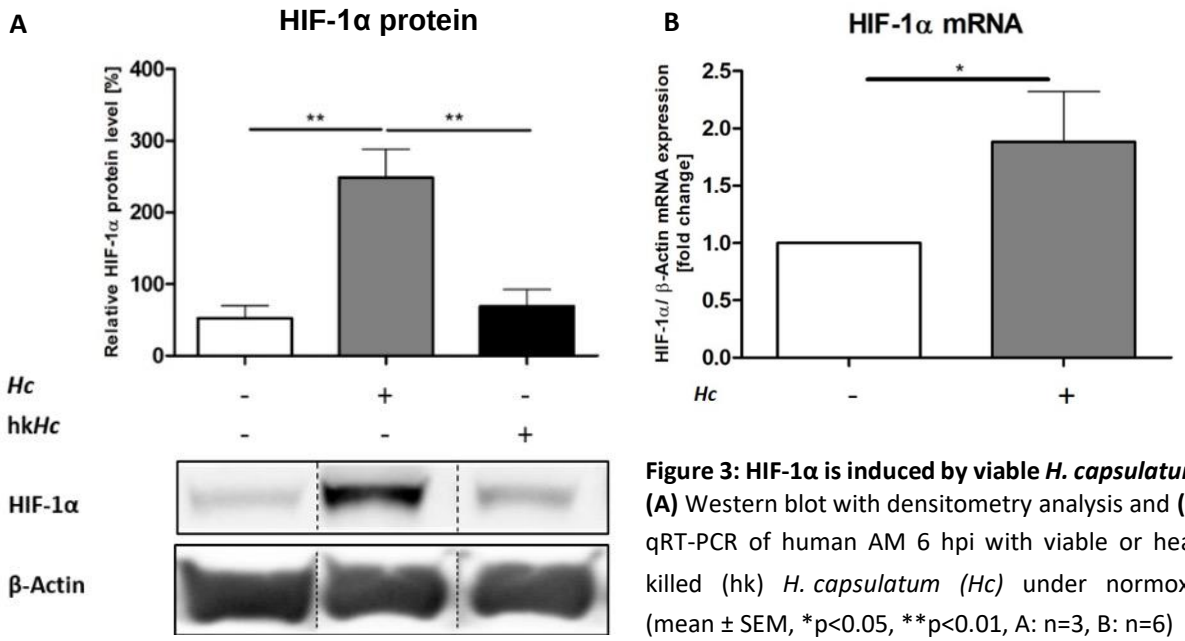

Figure 3: HIF-1α is induced by viable *H. capsulatum*. **(A)** Western blot with densitometry analysis and **(B)** qRT-PCR of human AM 6 hpi with viable or heat-killed (hk) *H. capsulatum (Hc)* under normoxia (mean ± SEM, *p<0.05, **p<0.01, A: n=3, B: n=6)

Protein levels of HIF-1α are significantly higher in alveolar MΦ infected with viable *H. capsulatum* compared to control cells or those exposed to heat-killed *H. capsulatum* (Figure 3A). Therefore, viability of the pathogen seems to be necessary to elevate HIF-1α protein levels. Also, infected alveolar MΦ show twice the amount of HIF-1α mRNA compared to uninfected control cells (Figure 3B).

One of the main functions of HIF-1α is to modulate the expression of various genes to allow cell adaptation. It has been shown in human MDMΦ to modulate expression of genes involved in glycolysis, pro-inflammation or vascularization. In addition to the upregulation of its protein levels, HIF-1α needs to translocate to the nucleus and dimerize with the constitutively expressed HIF-1β subunit to exert its function as a transcription factor, which I showed by an immunofluorescent approach, visualizing the nuclear accumulation of HIF-1α.

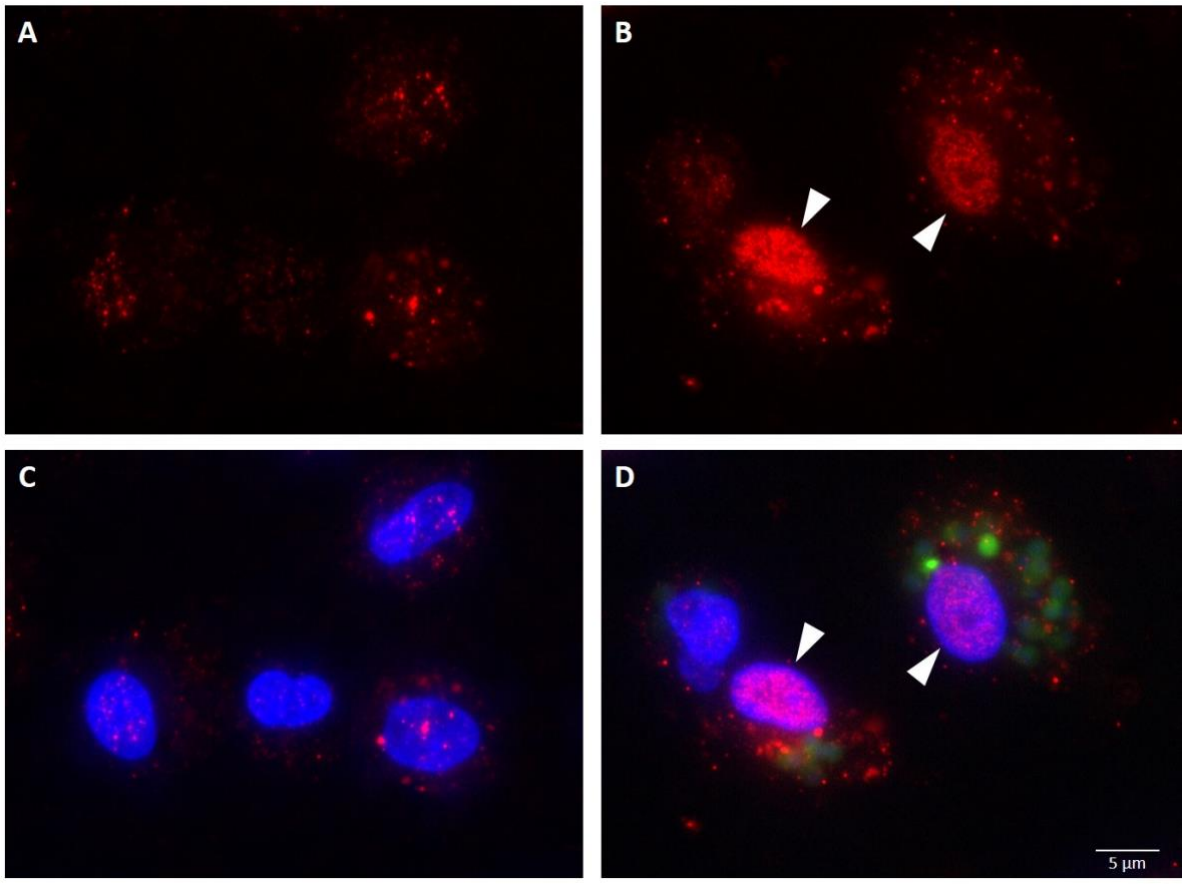

Figure 4: Location of HIF-1α within AM.
Immunofluorescence pictures of uninfected control cells **(A,C)** and *H. capsulatum* infected AM **(B,D)** 6 hpi. Cells were stained for HIF-1α (red), DAPI (blue) was used as nuclear counter stain, *H. capsulatum* yeasts were labeled with CFSE (green) prior to infection. (white arrows highlight nuclei positive for HIF-1α, scale bar= 5 µm, images representative of three experiments)

After 6 h of infection with *H. capsulatum,* alveolar MΦ have ingested numerous intracellular yeasts (Figure 4B, D) and additionally show areas of highly intense HIF-1α staining that correlate with the nuclear DAPI stain. As opposed to that, uninfected control cells show diffuse staining of HIF-1α throughout the complete cell (Figure 4A, C).

3.1.2 Influence of hypoxia and chemical HIF-1α stabilizers on HIF-1α protein levels

H. capsulatum infection elevates the levels of HIF-1α in alveolar MΦ by modulating its gene expression and stabilization of the abundant protein. The effect of hypoxia on HIF-1α was analyzed with and without *H. capsulatum* infection and was compared to uninfected, normoxic conditions. Further, the effect of chemical HIF-1α stabilization by DMOG (100µM) was investigated for the same conditions. DMOG inhibits the degradation of HIF-1α by inhibiting the O_2-dependent PHDs and thereby leads to HIF-1α protein accumulation. As explained in chapter 1.5 it allows a more specific investigation of the effects attributable to the changes in HIF-1α levels.

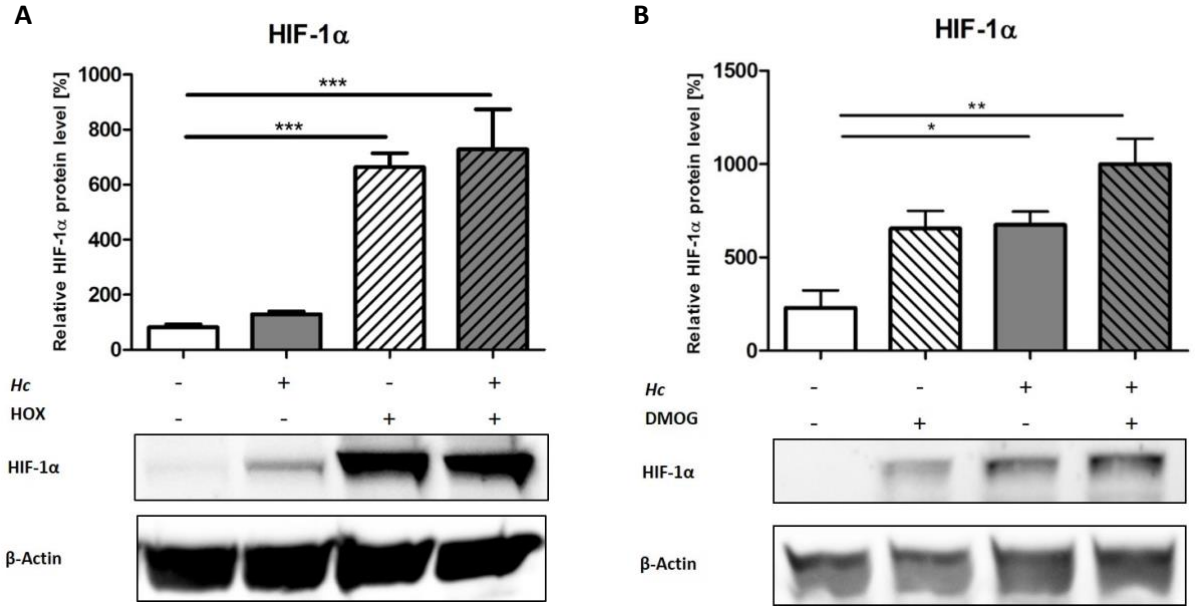

Figure 5: HIF-1α protein levels are elevated by hypoxia and DMOG
Western blot analysis of AM under **(A)** normoxia and hypoxia (HOX) with or without infection or **(B)** DMOG treatment with or without infection for 6 h. (mean ± SEM, *p<0.05, **p<0.01, ***p<0.001, **A** n=4, **B** n=3)

Hypoxia lead to a significant 7-fold increase in HIF-1α signal compared to normoxic control cells and infected, normoxic cells. Infecting the hypoxic cells did not lead to an additional increase in HIF-1α (Figure 5A). DMOG treatment also lead to an intensification of HIF-1α signal that is comparable to that of infected cells and was 3 times higher than control cells. Additional infection of DMOG treated cells lead to a further increase in HIF-1α protein without reaching statistical significance compared to infection alone (Figure 5B).

3.2 Host cell metabolism and pro-inflammatory response during *H. capsulatum* infection

In the case of MΦ, cellular activation is a driver of inflammation, high glycolytic activity, and is associated with HIF-1α. The results in this chapter are to elucidate how the infection with *H. capsulatum* alters the activation state of alveolar MΦ in terms of metabolism and inflammatory gene expression and in what way this response is modulated by HIF-1α. Metabolic experiments were carried out in murine alveolar MΦ.

First, it was necessary to confirm that the basic mechanisms shown before also apply in the murine system. Therefore, HIF-1α protein and mRNA levels in *H. capsulatum* infected murine alveolar MΦ at same infection dose as in the human alveolar MΦ were analyzed 6 hpi. Murine alveolar MΦ were treated with 50 µM IOX2, an inhibitor of PHD2. Its potential to stabilize HIF-1α is shown in Figure 6A.

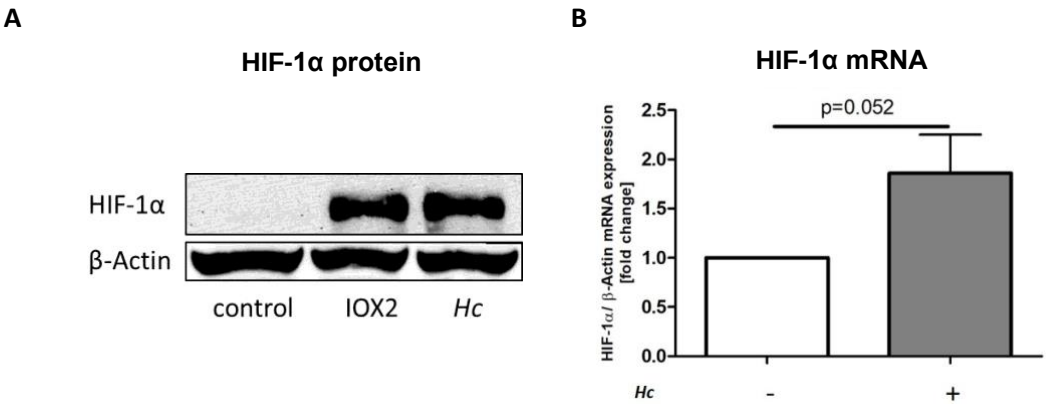

Figure 6: HIF-1α protein and mRNA levels in murine AM.
Western blot **(A)** and qRT-PCR **(B)** analysis of murine AM 6 hpi. For protein levels 50 µM IOX2 was used as a positive control. (**A** representative of n=3; **B** fold-change HIF-1α mRNA levels, mean ± SEM, n=6)

Murine alveolar MΦ also show an enhancement of HIF-1α protein signal in western blot analysis, comparable to the one induced by the HIF-1α stabilizer IOX2. HIF-1α was undetectable in uninfected control cells (Figure 6A). For HIF-1α mRNA levels in murine alveolar MΦ there was a tendency of enhanced gene expression with borderline significance (Figure 6B). Based on this, murine alveolar MΦ were used for metabolic analysis. In the following, murine and human data will therefore be shown in parallel as indicated.

3.2.1 Mitochondrial respiration in murine alveolar macrophages

Host cell metabolism is known to be an indicator of the activation state of immune cells. To determine the influence of the infection with *H. capsulatum* on the mitochondrial respiration of murine alveolar MΦ, the oxygen consumption rate (OCR) was measured. Adding Oligomycin, FCCP and Antimycin A/ Rotenone allowed the calculation of the basal respiration, ATP production and maximal respiration as indicated in chapter 2.2.6.1. Further, the non-mitochondrial respiration and proton leak were

calculated (data not shown). Heat-killed *H. capsulatum* was used to differentiate between effects that are solely mediated by phagocytosis and receptor binding and active modulation by the pathogen.

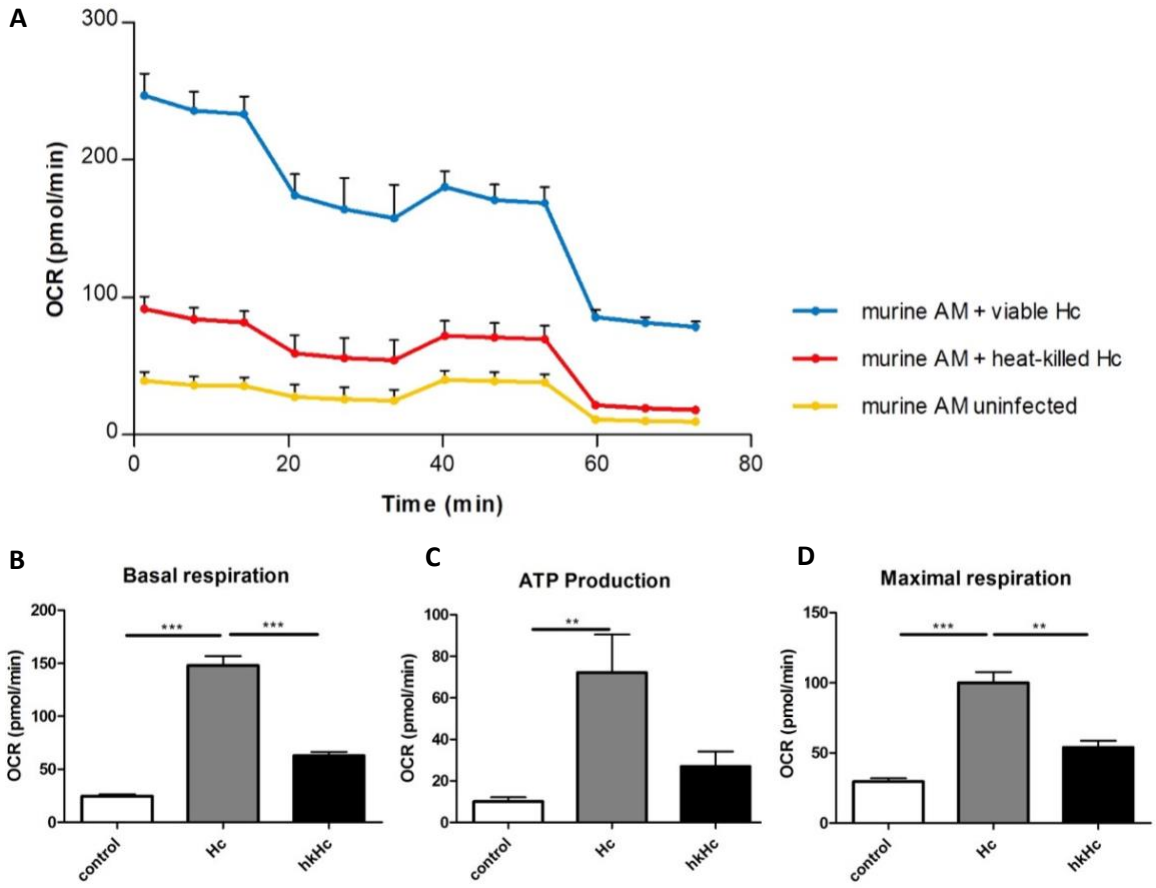

Figure 7: *H. capsulatum* activates mitochondrial respiration in murine AM.
Mito Stress Test Profile of murine AM **(A)** 6 hpi. Basal respiration **(B),** ATP Production **(C)** and Maximal respiration **(D)** are displayed as bar graphs. (mean ± SEM, **p<0.01, ***p<0.001, n=4)

Infection with viable *H. capsulatum* lead to a significant increase in basal respiration, ATP production and maximal respiration. Changes induced by heat-killed *H. capsulatum* were not significant compared to the control (Figure 7).

3.2.2 Glycolysis in murine alveolar macrophages

Glycolysis has implications for cellular activation. For determination of the functional glycolysis, the extracellular acidification rate (ECAR) was measured. With the help of glucose, oligomycin and 2-deoxyglucose (2-DG) the parameters glucose metabolism, spare capacity and non-glycolytic acidification were calculated as indicated in chapter 2.2.6.2. Conditions tested were the same as for the mitochondrial respiration. Because HIF-1α is often described as a driver to activate glucose metabolism, the experiments were also performed with alveolar MΦ from HIF-1α myeloid knock-out mice.

3.2.2.1 Functional glycolysis in HIF-1α competent alveolar macrophages

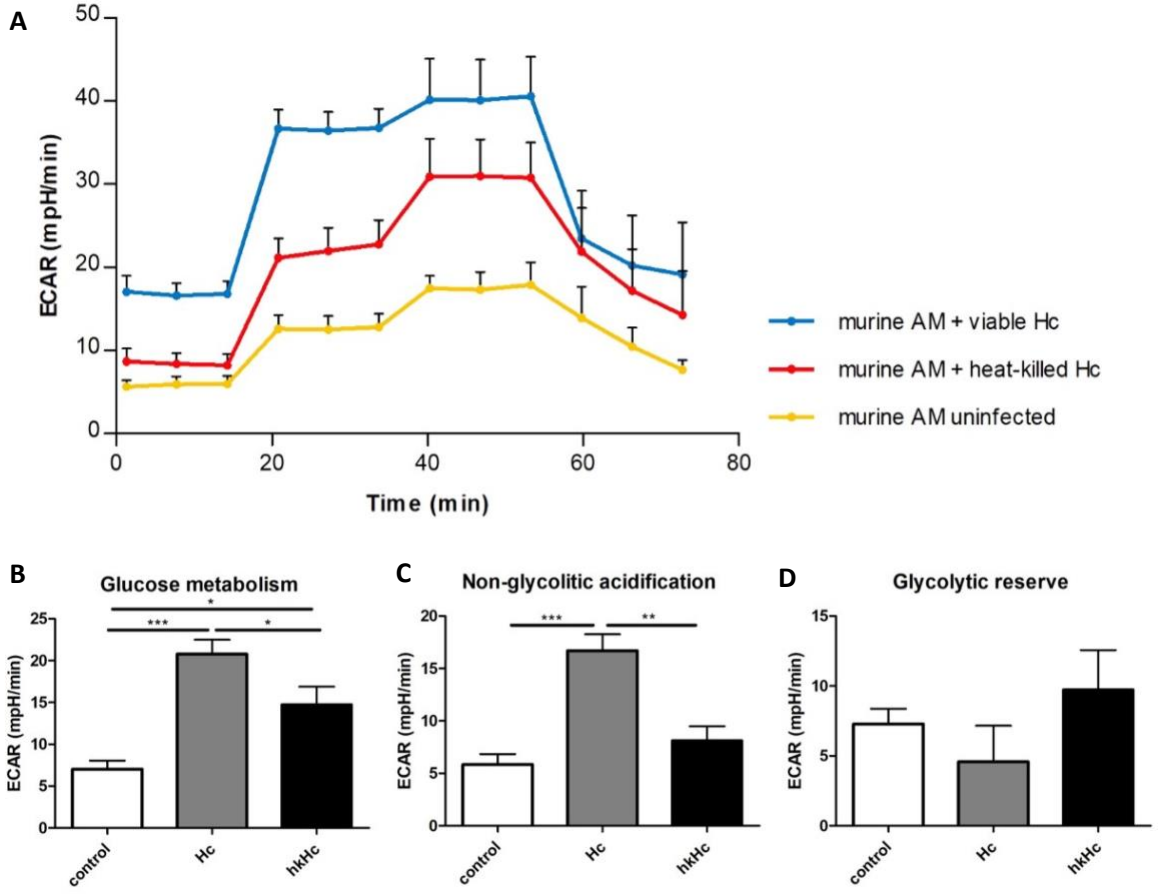

Figure 8: *H. capsulatum* activates glycolysis in murine AM.
Glyco Stress Test Profile of murine AM 6 hpi **(A)**. Glucose metabolism **(B),** Non-glycolytic acidification **(C)** and Glycolytic reserve **(D)** are displayed as bar graphs. (mean ± SEM, *p<0.05, **p<0.01, ***p<0.001, n=5)

Exposing murine alveolar MΦ to heat-killed *H. capsulatum* caused an increase in their glucose metabolism compared to the control, whereas no change could be observed for the non-glycolytic acidification rate and the glycolytic reserve. Infection with viable *H. capsulatum* lead to an even stronger increase in glucose metabolism. The non-glycolytic acidification rate was also elevated, whereas the glycolytic reserve was not influenced by the pathogen (Figure 8).

3.2.2.1 Functional glycolysis in HIF-1α knock-out alveolar macrophages

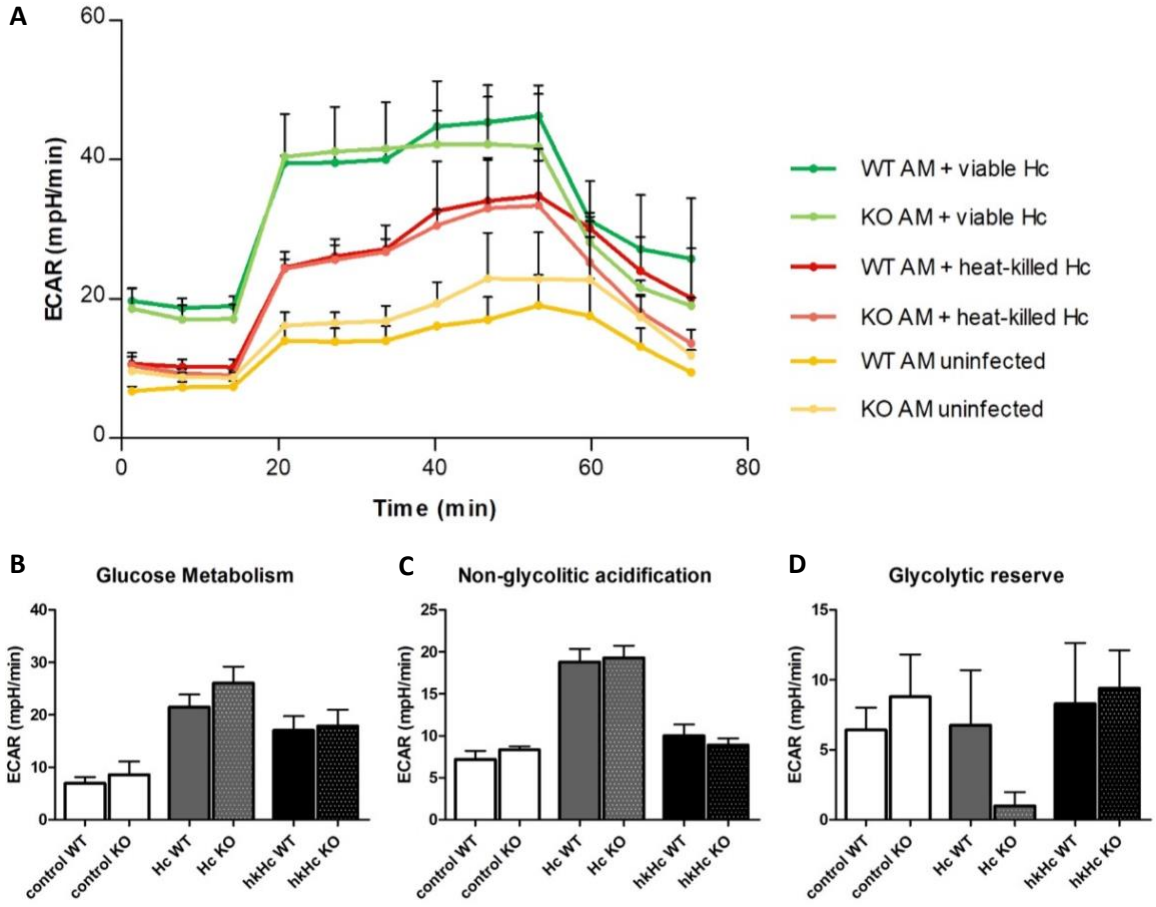

Figure 9: Glycolysis in HIF-1α deficient murine AM.
Glyco Stress Test Profile of wild type (WT) and HIF-1α$^{-/-}$ (KO) murine AM 6 hpi **(A)**. Comparing the ECAR for Glucose metabolism **(B),** Non-glycolytic acidification **(C)** and Glycolytic reserve **(D),** results for WT and HIF-1α $^{-/-}$ conditions are shown side by side in the bar graphs. (mean ± SEM, n=3 for WT and KO)

The absence of HIF-1α did not lead to changes in glucose metabolism when compared to the respective condition in wild-type alveolar MΦ (Figure 9).

3.2.3 Glycolytic gene expression

To assess the transcriptional response, the expression of HIF-1α associated glycolytic genes was analyzed. GLUT-1 encodes for a glucose transporter and PDK1 encodes an enzyme leading to the phosphorylation and inactivation of pyruvate dehydrogenase and thereby a reduction of pyruvate derived acetyl-CoA for the mitochondrial respiration. Determination of gene expression was done in human and murine alveolar MΦ.

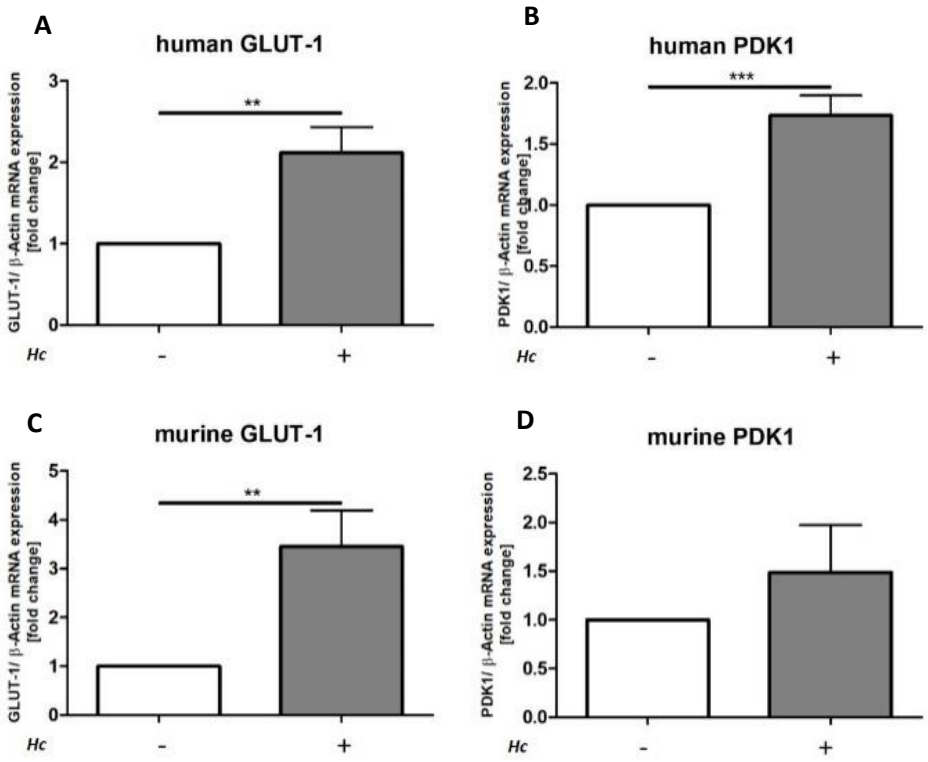

Figure 10: Expression of glycolytic genes is enhanced in AM by infection
GLUT-1 **(A,C)** and PDK1 **(B,D)** mRNA levels are shown for human **(A,B)** and murine **(C,D)** AM 6 hpi. (mean ± SEM, **p<0.01, ***p<0.001, n=6)

Both, human and murine alveolar MΦ infected with *H. capsulatum* showed upregulated GLUT-1 and PDK1 expression (Figure 10). However, changes in PDK1 regulation in mice did not reach significance.

The expression of these glycolytic genes is known to be HIF-1α associated. Hence, the glycolytic gene expression was investigated by treating uninfected and infected human alveolar MΦ with DMOG to understand how chemical HIF-1α stabilization influences the cellular activation state in terms of glycolytic gene expression. This may help to understand if alveolar MΦ respond differently to these stimuli than other previously investigated types of MΦ. The changes in HIF-1α levels induced by DMOG are shown in Figure 5B.

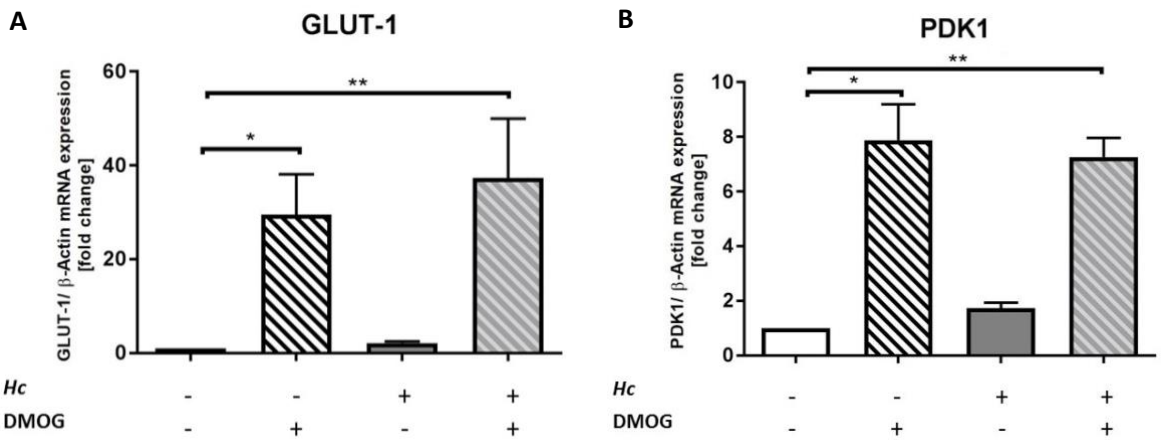

Figure 11: Expression of glycolytic genes is driven by DMOG in human AM
GLUT-1 **(A)** and PDK1 **(B)** mRNA levels in human AM 6 hpi are shown for HIF-1α stabilizer treatment and were compared to control cells and treated cells with additional infection (mean ± SEM, *p<0.05, **p<0.01, n=5)

Treating alveolar MΦ with DMOG lead to a significant upregulation of GLUT-1 and PDK1 expression, which could not be further enhanced by infecting the treated cells (Figure 11).

3.2.4 Pro-inflammatory gene expression

Cellular activation may not only lead to metabolic changes, but also to an altered cytokine response. For that purpose, the expression of the pro-inflammatory genes TNF-α and IL-1β was investigated in human and murine cells during infection. Chemical HIF-1α stabilization has in different cases been described to lead to a further enhancement, especially of IL-1β expression. Therefore, human alveolar MΦ were also treated with DMOG and murine alveolar MΦ with IOX2.

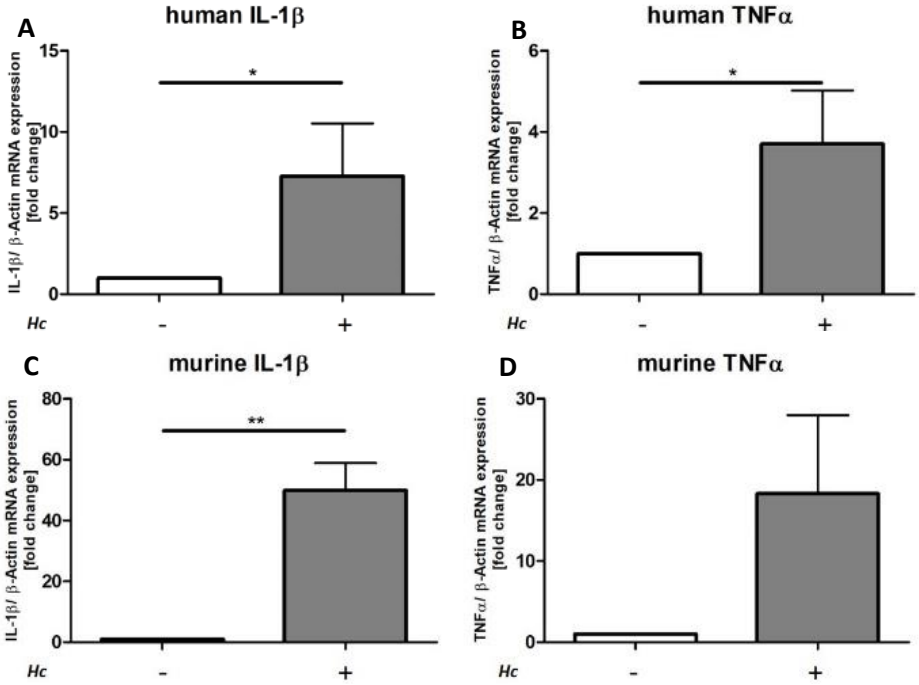

Figure 12: Expression of pro-inflammatory cytokines in *H. capsulatum* infected AM
IL-1β **(A,C)** and TNF-α **(B,D)** mRNA levels are shown in human **(A,B)** and murine **(C,D)** AM infected with *H. capsulatum* and were compared to control cells 24 hpi (mean ± SEM, *p<0.05, **p<0.01, n=4).

Comparing infected to uninfected cells, higher expression of IL-1β was induced in human and murine alveolar MΦ (Figure 12). For TNF-α, elevation was only significant in the human model. Therefore, influence of DMOG and IOX2 was tested for IL-1β. Herein, the treatment along with the infection did not induce significantly higher levels in the human model when comparing infected cells with and without DMOG treatment (Figure 13A). In the murine alveolar MΦ the combination of infection and treatment with IOX2 lead to a significant increase in IL-1β expression compared to the infected but untreated cells (Figure 13B).

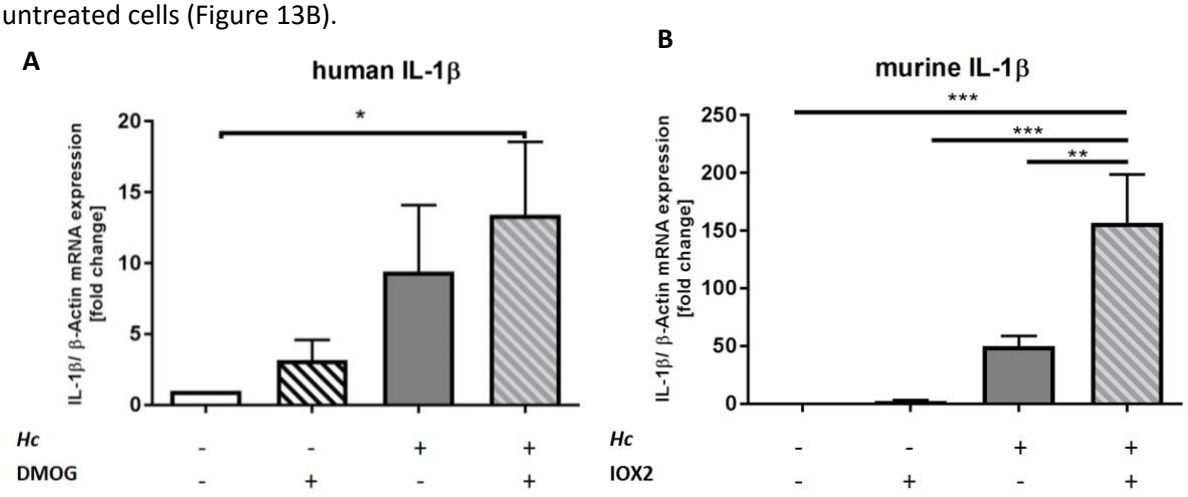

Figure 13: Alteration of IL-1β expression by HIF-1α stabilization in AM
IL-1β mRNA levels in AM treated with HIF-1α stabilizers and additional infection for human AM **(A)** and murine AM **(B)** 24 hpi**.** Results were compared to HIF-1α stabilizer treatment alone and infection alone (mean ± SEM, *p<0.05, **p<0.01, ***p<0.001, n=4).

3.3 Intracellular survival of *H. capsulatum* in alveolar macrophages

One of *H. capsulatum's* remarkable features is the ability to persist inside MΦ. Especially from a clinical point of view, strategies to overcome this persistence are of particular importance. In this work I addressed hypoxia, HIF-1α and glycolysis as possible targets to influence intracellular survival.

3.3.1 Survival of *H. capsulatum* under hypoxia and HIF-1α stabilization

It has been shown that hypoxia enables MDMΦ to elicit fungicidal activity against *H. capsulatum.* This fungicidal activity could also be mimicked by HIF-1α stabilizers DMOG and IOX2. Therefore, the influence of hypoxia was tested in human alveolar MΦ and the influence of HIF-1α stabilizers tested in both human and murine alveolar MΦ.

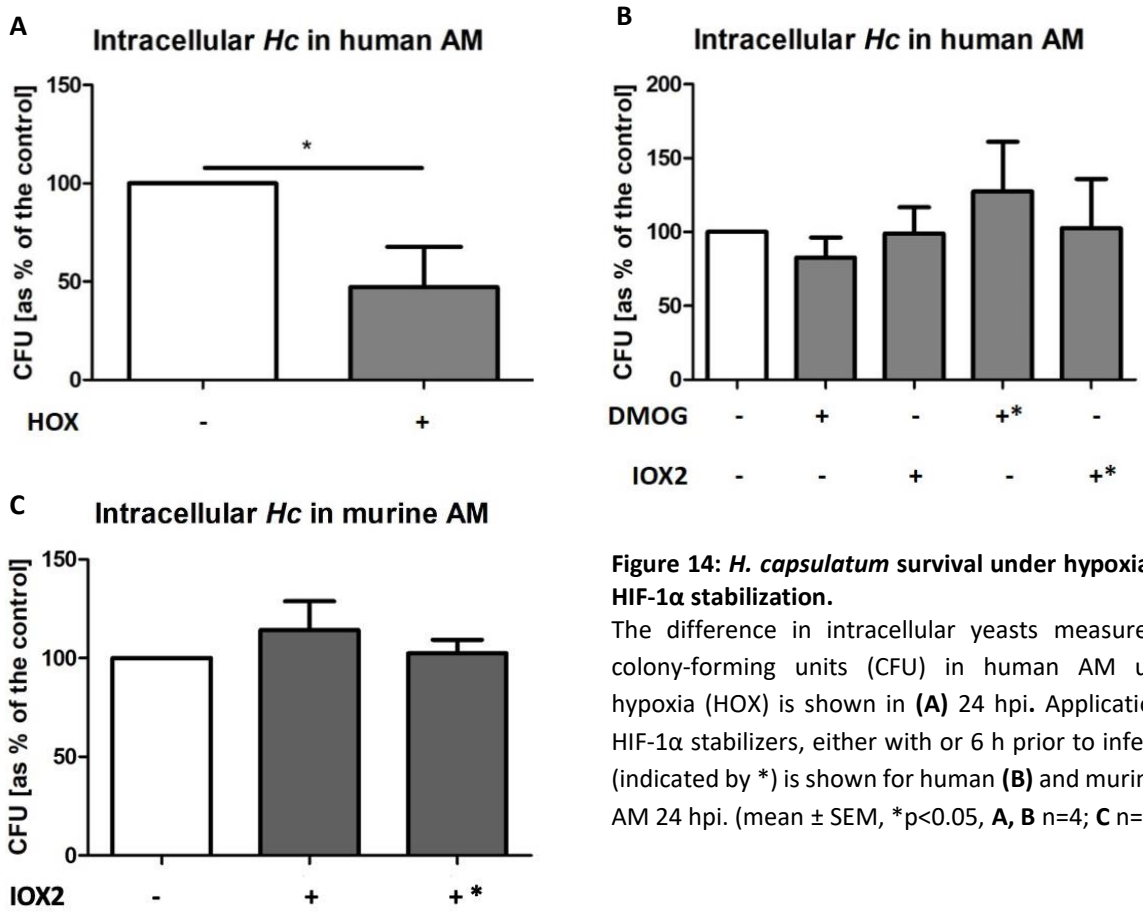

Figure 14: *H. capsulatum* survival under hypoxia and HIF-1α stabilization.
The difference in intracellular yeasts measured as colony-forming units (CFU) in human AM under hypoxia (HOX) is shown in **(A)** 24 hpi**.** Application of HIF-1α stabilizers, either with or 6 h prior to infection (indicated by *) is shown for human **(B)** and murine **(C)** AM 24 hpi. (mean ± SEM, *p<0.05, **A, B** n=4; **C** n=3).

Hypoxia significantly reduced fungal burdens by 53 ± 20% 24 hpi (Figure 14A). However, neither DMOG nor IOX2 could reduce fungal burdens (Figure 14B). This was regardless of whether drugs were applied with or 6 h prior to the infection. Results were confirmed by 18s RNA levels of *H. capsulatum* (data not shown). In murine alveolar MΦ, the influence of IOX2 on *H. capsulatum* survival was tested and again no difference was found (Figure 14C).

3.3.2 Survival of *H. capsulatum* under inhibition of host-cell glycolysis

Glycolysis has in different infection models been described as a necessary cellular activation mechanism to contain infection. Accordingly, this study shows higher expression of glycolytic genes and an activated functional glycolysis in infected cells (Figure 8, Figure 10). To investigate the role of glycolysis for intracellular *H. capsulatum* survival, alveolar MΦ were treated with different doses of the glycolysis inhibitor 2-DG which binds to and inhibits the hexokinase. To exclude direct effects of 2-DG on *H. capsulatum,* yeasts were incubated in medium containing 2-DG for 24 h. To exclude the possibility of yeasts not being phagocytized or released during the course of infection, supernatants of infected alveolar MΦ were analyzed for viable *H. capsulatum*.

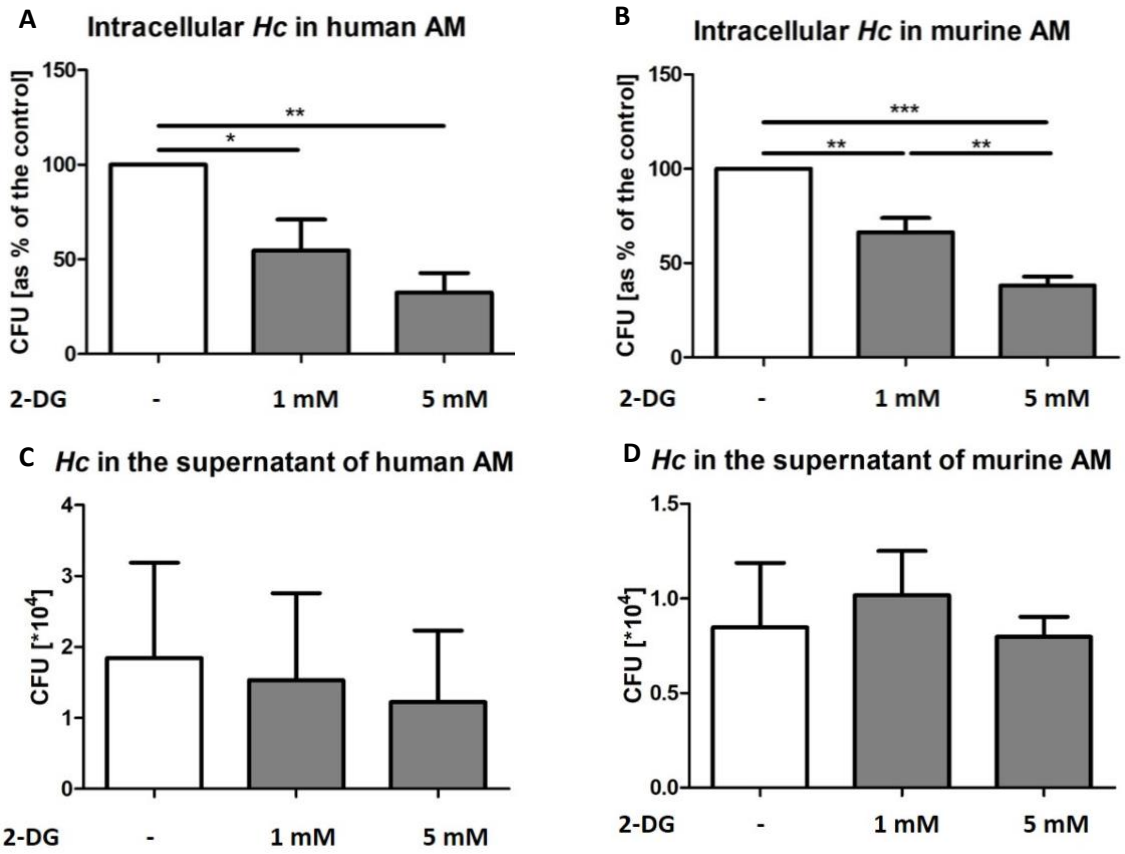

Figure 15: *H. capsulatum* survival under 2-DG treatment
A, B show the difference in intracellular viable yeasts recovered from AM induced by 2-DG treatment in human **(A)** and murine **(B)** AM 24 hpi. The number of free yeasts recovered from the supernatant is shown in **C** (human) and **D** (murine)**.** (mean ± SEM, *p<0.05, **p<0.01, ***p<0.001 **A, B, C** n=4, **D** n=3).

Applying 2-DG for 24 h to the culture media did not have a direct effect on *H. capsulatum* (data not shown). Also, the number of yeasts found in the supernatant did not differ, meaning there was no deficient phagocytosis or pathogen release from dying cells (Figure 15 C, D). When alveolar MΦ were treated with 2-DG before infection, the number of intracellular yeasts decreased, in a dose dependent manner in both human and murine alveolar MΦ (Figure 15 A, B).

To have a visual correlate for the decreased colony-forming units (CFU) found in the plating assays, alveolar MΦ were analyzed by electron microscopy. Images of uninfected alveolar MΦ were compared to those of infected alveolar MΦ. As seen in Figure 16A, vesicles in uninfected alveolar MΦ hardly exceed the size of 1 µm, which allows to differentiate them from *H. capsulatum* yeast phagosomes, that range from 2 µm to 5 µm (Figure 16B-D). To test for the general ability of alveolar MΦ to degrade the yeasts and to display what degraded yeasts look like intracellularly, heat-killed *H. capsulatum* treatment (Figure 16C) was compared to the infection with viable *H. capsulatum* infection (Figure 16B). Alveolar MΦ infected with viable yeasts show oval phagosomes harboring intact *H. capsulatum* and a typical halo around the yeast (Figure 16B). These are characterized by a solid (grey) phagosome content, showing the yeast, which is surrounded by a lighter halo. Alveolar MΦ exposed to heat-killed *H. capsulatum* show phagosomes of similar size (Figure 16C). Opposed to the viable infection the phagosome content appears to be demolished. Yeasts do not appear as solid grey anymore and a halo is either entirely absent or fading. Those cells pre-treated with the glycolysis inhibitor 2-DG show a mixed picture of phagosomes (Figure 16D). While some appear as solid grey and halo surrounded, resembling the phagosomes found in Figure 16B, many others seem to contain debris like the phagosomes with the heat-killed *H. capsulatum* in Figure 16C.

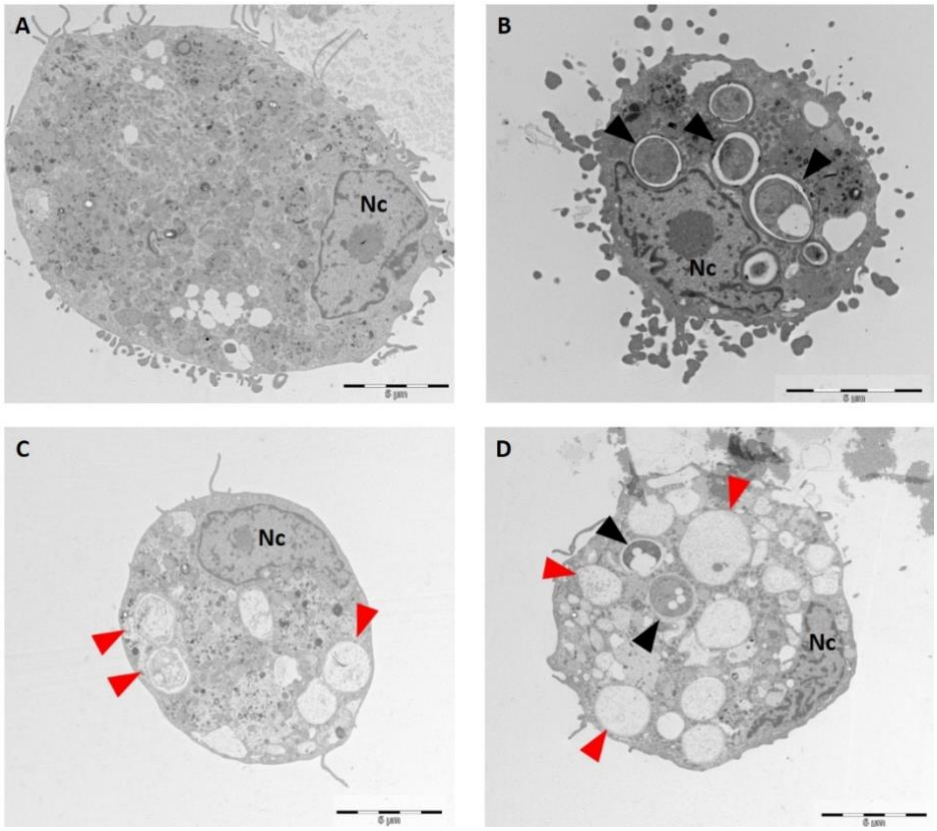

Figure 16: AM with inhibited glycolysis degrade *H. capsulatum*.
Electron microscopy pictures show uninfected AM **(A),** AM infected with viable *Hc* **(B),** AM exposed to heat-killed *Hc* **(C)** and 2-DG treated AM infected with *Hc* **(D)** 24 hpi**.** (Nc = nucleus, scale bars = 5 µm respectively, black arrows show phagosomes with viable yeasts, red arrows show demolished yeast-sized phagosomes, representative of n=3 experiments)

4. Discussion

4.1 Fungal infections induce higher levels of HIF-1α

While HIF-1α is traditionally seen as a regulator to allow cell homeostasis under hypoxic conditions (J.-W. Lee et al. 2004), its functions in inflammation, innate immunity and infection are emerging (Hellwig-Bürgel et al. 2005; Tannahill et al. 2013; Scholz and Taylor 2013). Despite the predominating investigations in bacterial infections (Zinkernagel et al. 2007), HIF-1α's importance in fungal infections is coming into focus (Friedrich et al. 2017). In *Aspergillus fumigatus* (Shepardson et al. 2014) and *Candida albicans* (Fan et al. 2015) infections, the notion for a functioning HIF-1α response in order to ensure host protection is described. In line with that, host cells show augmented HIF-1α protein levels when exposed to these fungi.

Accordingly, results presented here showed higher levels of HIF-1α protein in the infected tissue specific alveolar MΦ (Figure 3A), allowing comparisons to other studies investigating HIF-1α in the context of *H. capsulatum* infections. In this respect, our work group has lately shown HIF-1α stabilization *in vivo* and *in vitro* as a protective factor against *H. capsulatum* on the host's side. *In vivo,* myeloid HIF-1α knockout C57BL/6 mice succumbed to sublethal doses of *H. capsulatum* (Fecher et al. 2016). *In vitro,* Friedrich showed that HIF-1α stabilizers improve pathogen clearance from MΦ and thereby blazed the trail for targeting HIF-1α pharmacologically (Friedrich 2016). Since these experiments were carried out in MDMΦ, it was of great importance to find out whether or not the same effect is true for alveolar MΦ, which represent the first line of defense against *H. capsulatum*. To lay ground for pharmacological experiments the range and mode of HIF-1α modulation by the pathogen itself was investigated.

4.1.1 Transcriptional HIF-1α induction

This study shows that there are higher levels of HIF-1α mRNA in infected compared to uninfected alveolar MΦ, indicating transcriptional regulation of the *hif1a* gene (Figure 3B, Figure 6B). Numerous known factors influence the *hif1a* gene expression. While autoinduction is limited to tumor cells (Koslowski et al. 2010), infections involve the PI3K/Akt pathway. *H. capsulatum* can be recognized through VLA-5 by DCs, which activates PI3K/Akt (B.-H. Lee and Ruoslahti 2005). Via mTOR this has been shown to cause a higher expression of *hif1a* (Giaccia et al. 2003). But since only DCs and not MΦ sense *H. capsulatum* through VLA-5, this is unlikely to be the reason for higher *hif1a* expression here (Gomez et al. 2008). However, another prominent inducer – NF-κB – is more likely to influence *hif1a* expression in this scenario. NF-κB induces expression of *hif1a* by its subunit RelA binding to a conserved κB site in the promoter region (Rius et al. 2008). Cytokines like TNF-α and IL-1β, which are highly expressed in infection experiments (Figure 12), are described to enable the nuclear translocation of NF-κB subunits

by activation of IκB kinase complex (IKK) (Hoesel and Schmid 2013; Serasanambati and Chilakapati 2016). Further matching the results presented here, MΦ recognize *H. capsulatum* through Dectin-1 and complement receptor (CR) 3 (CD11b/CD18). Dectin-1 and CR3 engage the Syk pathway by activating the Syk kinase (Jr-Shiuan et al. 2010). Takada et al. showed that Syk signaling is also involved in the activation of NF-κB (Takada et al. 2003). Apart from that, *H. capsulatum* cell wall protein Yps3p is recognized by the toll-like receptor 2 (TLR2). Via engagement of further prominent signaling molecules like MyD88 or IRAK1, TLR2 also activates the canonical pathway of NF-κB leading to the nuclear translocation of RelA (Sabroe et al. 2003; Aravalli et al. 2008). All these interconnections strongly suggest a role for NF-κB in the induction of higher HIF-1α mRNA levels seen in above presented experiments. Unfortunately, results from preliminary experiments did not allow valid conclusions going in either direction (data not shown). Further investigation of NF-κB is necessary to gain a better understanding of the mode of HIF-1α induction and would then provide another knob to turn for experimental HIF-1α manipulation.

4.1.2 Post-transcriptional HIF-1α induction

Besides the transcriptional regulation of the *hif1a* gene, post-transcriptional limitation of the proteasomal degradation leads to HIF-1α protein accumulation during infection as well as under hypoxia (Figure 3A, Figure 5A). Interestingly, additionally infecting alveolar MΦ with *H. capsulatum* under hypoxic conditions did not lead to higher HIF-1α levels than hypoxia alone (Figure 5A), which is in contrast to the findings made in MDMΦ (Friedrich 2016). This might indicate that hypoxia is a much stronger stimulus for HIF-1α induction in alveolar MΦ than in MDMΦ. While MDMΦ represent phagocytes that act systemically, they experience continuous variations in oxygen availability. For example, the oxygen depleted venous blood has an average partial O_2 pressure (pO2) of 40 mmHg. Alveolar MΦ however are in general exposed to an O_2 rich environment in the alveolar airspace with up to 100 mmHg pO_2 (Golenhofen, 2011). This could explain the greater need for adaptation to hypoxia in alveolar MΦ. Another explanation could be that alveolar MΦ as opposed to MDMΦ are much more reluctant towards *H. capsulatum* infection, since their main function is to dampen inflammatory stimuli with the aim to avoid massive pulmonary inflammation (Hussell and Bell 2014). Herein, preliminary experiments showed higher HIF-1α protein levels in MDMΦ compared to alveolar MΦ upon *H. capsulatum* infection, supporting the latter assumption (data not shown). Much alike the hypoxic conditions, pharmacological HIF-1α stabilizers, DMOG and IOX2, inhibit the PHDs (Jaakkola et al. 2001; Chowdhury et al. 2013). This mimics the HIF-1α increase. However, oxygen is in contrast to hypoxia still available. In experiments with human alveolar MΦ, DMOG was preferably used. This allows comparability to the data obtained in MDMΦ, where also DMOG was primarily used. In murine experiments IOX2 was preferred, because of its affinity to PHD2. This allows a more specific and clearer

HIF-1α protein enhancement compared to DMOG, which inhibits multiple PHDs (Berra et al. 2003; Chowdhury et al. 2013). Even though IOX2 may allow high specificity for the enhancement of HIF-1α protein, other groups argue that using DMOG comes closer to mimicking hypoxic environments than inhibitors with high PHD specificity (Chan et al. 2016), leaving the question of the best inhibitor a matter of how the experimental question is posed. Nonetheless, IOX2 and DMOG are appropriate mimicry for the hypoxic HIF-1α stabilization in the respective system as shown in the results (Figure 5B, Figure 6A).

The question of greater interest is the mode of HIF-1α stabilization during infection with *H. capsulatum*. Generally, HIF-1α stabilization due to oxygen scarcity is proposed for infection models, too. Werth et al. showed that HIF-1α levels increase during *in vitro* infection experiments due to higher O_2 consumption (Werth et al. 2010). Infection with *H. capsulatum* also showed a strongly increased mitochondrial activity (Figure 7). Therefore, O_2 availability likely decreases during *H. capsulatum* infection. In addition, an increased mitochondrial activity may also lead to higher concentrations of citric acid cycle intermediates, such as succinate. Succinate, which is the result of splitting CoA from succinyl-CoA, is a known inhibitor of PHDs and may provide another link between mitochondrial respiration and HIF-1α during *H. capsulatum* infection (Selak et al. 2005). However, not only mitochondrial respiration but also glycolysis links to the post-transcriptional stabilization of HIF-1α. As seen in Figure 8, glycolytic activity is upregulated during infection, which implies higher lactate levels, as lactate represents the end product of (an)aerobic glycolysis (Zech 2006). Lactate in return is converted into pyruvate via lactate dehydrogenase (LDH) B activity, which exhibits inhibitory effects on PHDs (Sonveaux et al. 2012). Other studies showed that supplementation with lactate or pyruvate, but not other intermediates of the citric acid cycle, lead to increased HIF-1α, indicating the effect is indeed through pyruvate and not consecutive degradation in the citric acid cycle (Lu et al. 2002). Apart from that, the iron binding capacity of *H. capsulatum*, which is mediated through siderophores, may influence the post-transcriptional HIF-1α modulation, since siderophores cause robust HIF-1α rises by inhibition of PHDs in bacterial infections. The secretion of siderophores is another *H. capsulatum* virulence factor (Hilty et al. 2011; Hartmann et al. 2018). Conclusively, both transcriptional and post-transcriptional mechanisms seem to lead to the HIF-1α protein accumulation during infection as presented in the results.

4.2 Influence of hypoxia and HIF-1α on the outcome of infection

To put the knowledge about HIF-1α stabilization and hypoxia to clinical use, its effects on the outcome of infection are crucial. The physiological response to infection is inflammation, which often leads to local hypoxia due to higher metabolic demands of present immune cells, limited substrate supply as a result of necrosis, thrombosis and compression and energy intensive replication of microorganisms (Eltzschig and Carmeliet 2011). It is tempting to speculate that hypoxia is not only a logical consequence of above-mentioned circumstances, but also an intended combat mechanism against microbial infections, because its effects can be highly beneficial for the host during infections. Especially the innate immune system is activated by hypoxia, so that MΦ are able to express higher levels of pro-inflammatory cytokines IL-1β or TNFα, and produce microbicidal NO under hypoxia (Hempel et al. 1996; Melillo et al. 1995). Also, they increase their phagocytic capacity (Anand et al. 2007). Additionally, their tissue adherence and anaerobic glycolytic capacity increase (Beck-Schimmer et al. 2001; Cramer et al. 2003). The experimental set-ups in this study use hypoxia to model the *in vivo* situation in granuloma and investigate if alveolar MΦ herein also control *H. capsulatum* growth. To untangle the complexity of hypoxia and to gain clinical advantage, experimental approaches are broken down to HIF-1α stabilization, as seen in the results presented here. For experiments with human alveolar MΦ, DMOG was preferably used to allow comparability to other models as explained in chapter 1.2. In the newly established model with murine alveolar MΦ, which provide a genetically stable model, IOX2 was used aiming to specifically investigate changes induced by higher HIF-1α levels. The applied doses of DMOG (100 µM) and IOX2 (50 µM) are commonly found in publications addressing HIF-1α (Acosta-Iborra et al. 2009; Deppe et al. 2016).

Under hypoxia, human MDMΦ were able to degrade viable *H. capsulatum* yeasts, while they were susceptible to infection under normoxia. Most importantly, this effect could also be observed under chemical HIF-1α elevation (Friedrich 2016). Whereas alveolar MΦ also showed lower fungal burdens under hypoxia as compared to normoxia (Figure 14A), pharmacological HIF-1α stabilization could not mimic this effect and showed same fungal burdens in treated and untreated alveolar MΦ (Figure 14B,C). This was valid for both HIF-1α stabilizers DMOG and IOX2. Since this finding was consistent in the human and murine system, it is likely due to the tissue specific type of MΦ. Reasons for the different response of alveolar MΦ and MDMΦ to pharmacological HIF-1α stabilization are most likely in the different nature of the cell types. Generally, alveolar MΦ tend to limit inflammatory responses and promote tissue repair instead of fueling inflammation (Murray and Wynn 2011). This may explain why the pro-inflammatory cytokine TNFα was only slightly elevated by pharmacological HIF-1α stabilizers during infection and an elevation of IL-1β was only seen in murine, but not in human alveolar MΦ (Figure 13). This was in contrast to the situation in MDMΦ, where HIF-1α stabilizers triggered a

massive release of pro-inflammatory cytokines (Friedrich 2016). This may indicate that – as determined by their nature – alveolar MΦ compared to MDMΦ fail to mount an adequate pro-inflammatory response under HIF-1α stabilization. Concluding from this, HIF-1α stabilizers as a pharmacological approach in Histoplasmosis treatment would not directly strengthen alveolar MΦ as the first line of defense. Another interesting approach to explain the difference between alveolar MΦ and MDMΦ are the metabolic changes observed under chemical HIF-1α stabilization. Herein, MDMΦ showed a diminished glycolytic activity when treated with DMOG (Friedrich 2016). As discussed in chapter 4.4 glycolysis inhibitors lead to lower fungal burdens in alveolar MΦ, while the effects of HIF-1α stabilizers on glycolysis have not been investigated yet.

For the decreased *H. capsulatum* CFUs under hypoxia (Figure 14A), it may be speculated that hypoxic conditions drive *H. capsulatum* into a state of dormancy, which results in less active yeasts in terms of replication. This concept is established in *M. tuberculosis* infection, where hypoxia and latent infections are linked (Rustad et al. 2008). *H. capsulatum* is hindered in its replicative activity under hypoxia and has a specific set of genes activated by srb1 under hypoxia. If this represents a more resilient state is currently unclear (DuBois et al. 2016). Conclusively, hypoxia gives MΦ an edge over *H. capsulatum* in terms of infection control that is in the case of alveolar MΦ not due to HIF-1α stabilization and likely a results of hindered *H. capsulatum* replication under hypoxia. Also, it possibly allows the pathogen to evade eradication.

Another interesting hypothesis is that alveolar MΦ function as immunological gate keepers that mount a systemic rather than a local inflammatory response, shorten bone-marrow transition time of monocytes and perpetuate their pulmonary infiltration (Ishii et al. 2005). A potent trigger for this systemic response by alveolar MΦ is alveolar hypoxia (Gonzalez et al. 2007). Elucidating the role of HIF-1α in this could be of great importance, as it would give a better understanding how HIF-1α and its pharmacological stabilization shape the systemic response to pulmonary infections and hypoxia. Generally, the investigation of HIF-1α manipulation with PHD inhibitors should be approached *in vivo* to test its properties as a therapeutic tool.

4.3 Intracellular infections shape the immunometabolism of the host cell

While pathogens need to adapt to hypoxic environments, the interaction with the host cell's metabolism is another crucial step for creating their intracellular niche. Especially in the context of infection, our perception of metabolism has changed throughout the years: From seeing metabolism as the energy supplier in catabolism and substrate supplier in anabolism over Otto Warburg's finding of the metabolic shift from OXPHOS to glycolysis in tumor cells to today's knowledge about its role in activation and polarization in immune cells (Arnheim and Rosenbaum 1904; Warburg 1925; Galván-Peña and O'Neill 2014).

The importance of metabolic adaptations has been shown in cancerous, metabolic and inflammatory diseases (Schertzer and Steinberg 2014). More specific for experiments presented here, the activation of MΦ has been associated with the Warburg-like shift from mitochondrial respiration to aerobic glycolysis (Galván-Peña and O'Neill 2014). Matching that, glucose metabolism in alveolar MΦ significantly increased during infection (Figure 8). Alike this, other intracellular pathogens such as *Chlamydia trachomatis* and *M. tuberculosis* also induce host glycolysis during infection (Ojcius et al. 1998; Gleeson et al. 2016). The mode of glycolysis activation is not fully understood. Recently, stimulation of TLRs was proven to induce a metabolic shift by inducing aerobic glycolysis and allowing ROS production from mitochondria (Krawczyk et al. 2010; West et al. 2011). Fungal cell wall structures have been shown to induce TLR signaling (Aravalli et al. 2008) and more specifically Cheng *et al.* showed that β-glucan induces glycolysis through the dectin-1 – Akt– mTOR – HIF-1α pathway (Cheng et al. 2014).

In the results presented here, not only glucose metabolism, but also the non-glycolytic acidification rate rose, which may be due to higher CO_2 production from a more active TCA cycle (Figure 7, Figure 8). Other metabolic assay experiments already identified CO_2 as the main contributor to non-glycolytic acidification (Pike Winer and Wu 2014).

An interesting point is the role of HIF-1α in this setting. HIF-1α induces a number of metabolically relevant genes. Among them are GLUT-1 and PDK1, which are both highly expressed during infection (Figure 10). GLUT-1 encodes for a glucose transporter increasing the cellular potential to take up glucose and provide substrate for glycolysis (Chen et al. 2001). PDK1 is an enzyme at the intersection of glycolysis and mitochondrial respiration. It phosphorylates and inactivates pyruvate dehydrogenase, preventing it from turning pyruvate into acetyl-CoA. Thereby, PDK1 down-regulates mitochondrial oxygen consumption (Kim et al. 2006). Nonetheless, results from *H. capsulatum* infections showed both metabolic pathways highly active despite a potent induction of HIF-1α during infection (Figure 3, Figure 7, Figure 8). This would have been expected to cause a Warburg like shift from OXPHOS to

glycolysis. To my knowledge, a similar effect has not yet been described in other pathogens but is consistent through different types of MΦ infected with *H. capsulatum* (data not shown). HIF-1α's main function in orchestrating the metabolic shift is shunting pyruvate away from the TCA cycle through PDK1. As mentioned above, the TCA cycle even in HIF-1α competent alveolar MΦ is more active during infection, despite PDK1 activation. This may imply that the fuel for the TCA cycle is not pyruvate but a different carbon source. Fatty acids and amino acids can enter the TCA cycle at different stages (Owen et al. 2002). The most prominent carbon source described in the activated state of MΦ, apart from glucose, is glutamine. Glutamine is the most abundant amino acid and besides glucose the most important energy source for proliferating immune cells (Gottfried et al. 2012). In the cellular energy balance, glutamine is described to account for a third of generated ATP in MΦ (Newsholme 2001). It is therefore possible that even though HIF-1α shunts pyruvate away from the TCA cycle through PDK1, other carbon sources like glutamine fuel the TCA cycle in infected MΦ and thereby lead to high O_2 consumption rates. A falsification of results by the pathogen's own metabolism is neglectable, as Friedrich showed that *H. capsulatum* recovered from MΦ shows very low glycolytic and mitochondrial activity (Friedrich 2016). A considerable influence of *H. capsulatum'*s own metabolism on the metabolic profiles therefore appears unlikely. To definitely answer this question, genetically modified *H. capsulatum* strains deficient for either glycolysis or OXPHOS are necessary and would at this point exceed the possibilities of our laboratory. Another explanation is induction of host OXPHOS through the pathogen itself. OXPHOS characterizes M2 MΦ (Tan et al. 2015). Like in many other intracellular pathogens, this rather anti-inflammatory MΦ type is favorable for *H. capsulatum* survival and OXPHOS may thereby contribute to lower release of pro-inflammatory cytokines (Verma et al. 2015; Muraille et al. 2014).

A further unexpected finding is that the absence of HIF-1α did not alter the glycolytic profile (Figure 9). This implies that either HIF-1α is irrelevant in the regulation of alveolar MΦ's metabolism during infection or that its absence is compensated. Possible explanations for this incongruence between HIF-1α levels followed by higher glycolytic gene expression and functional metabolism may be found in the experimental setting. HIF-1α influences are usually tested in cancer-conditions or knock-out experiments with no pathogenic organism present. *H. capsulatum* may therefore activate signaling pathways that work independently from HIF-1α. In line with that, Rodriguez-Prados *et al.* describe a number of stimuli that are potent to induce aerobic glycolysis even in absence of HIF-1α and may be relevant in *H. capsulatum* infections, like TLR-2 and TNF-α signaling (Rodríguez-Prados et al. 2010). Conclusively, the induction of HIF-1α dependent genes may corroborate glycolysis, but it is neither rate limiting as seen in HIF-1α $^{-/-}$ alveolar MΦ , nor does it enhance the glycolytic capacity during infection (Figure 9).

4.4 H. capsulatum exploits the host cell metabolism

While there was no influence of HIF-1α on the glycolytic phenotype of the host cell in the experimental results presented (Figure 9), glycolysis in return may influence HIF-1α levels. Tannahil et al. describe that applying 2-DG as a glycolysis inhibitor decreased the accumulation of HIF-1α protein (Tannahill et al. 2013). Even though this was not investigated in detail in this work, preliminary results show decreased HIF-1α protein levels in *H. capsulatum* infected alveolar MΦ treated with 2-DG compared to those left untreated (data not shown). This is very likely due to the lack of lactate caused by the inhibition of glycolysis, as discussed in chapter 4.1.2. The 2-DG doses used in the presented experiments are commonly used in studies addressing HIF-1α or infection models in MΦ (Tannahill et al. 2013; Gleeson et al. 2016)

Metabolic demands during infection do not only change for the host cell, but also for the pathogen inside the host cell. Intracellular as opposed to extracellular pathogens cannot rely on covering their nutritional demands with nutrients delivered to them by the circulation. Instead, they need to rely on their host cell to provide sufficient nutrient supply and sometimes they have to make their host cell provide nutrients. Inside the host cell, pathogens find themselves in vacuoles where they have to find strategies to access nutrients. Only few pathogens have evolved strategies to escape their vacuole and enter the host cell cytosol for nutrient supply (Ray et al. 2009). For all others, nutrients have to be brought into the vacuole, either via transporters synthesized by host or pathogen, or via fusion with other endocytic vesicles (Kirk and Lehane 2014; Drecktrah et al. 2007). In *H. capsulatum* a dependence on the host has been shown for various ions like iron, zinc and calcium (Winters et al. 2010; Hwang et al. 2008; Sebghati et al. 2000). However, little is known how *H. capsulatum* meets its energy demands. While in other pathogens the preferable energy source is identified (Abu Kwaik and Bumann 2015), in *H. capsulatum* speculations are on any available source of carbon (Garfoot and Rappleye 2016).

This study shows that inhibition of glycolysis leads to intracellular degradation and lower fungal burdens of *H. capsulatum* in alveolar MΦ (Figure 15, Figure 16). The dependence on glycolysis has been previously described in infections with *Salmonella enterica* and *Brucella abortus* (Bowden et al. 2009; Czyz et al. 2017). In the latter work, Czyz *et al.* could identify lactate as the critical carbon source that is provided by host MΦs' glycolysis and lacks in case of glycolysis inhibition. In this context, the findings by Gleeson et al., who could show that in *M. tuberculosis* infections the inhibition of glycolysis with 2-DG at same concentrations caused a 50- 100% increase in *M. tuberculosis* CFUs, provide a striking piece of literature, claiming the opposite effect to the results presented here (Gleeson et al. 2016). This comes as a particular surprise, as *M. tuberculosis* and *H. capsulatum* are often compared due to their intracellular lifestyle and slow replication rates.

The results on the intracellular survival of *H. capsulatum* in 2-DG treated MΦ (Figure 15) show that there has to be dependence on products created in the course of glycolysis, since 2-DG binds to and inhibits the hexokinase, the first enzyme of the glycolytic pathway. A misinterpretation of results due to diminished phagocytosis or release of *H. capsulatum* from apoptotic MΦ was ruled out by the numbers of free yeasts in the supernatants, which did not differ between treated and untreated alveolar MΦ (Figure 15). As 2-DG did not have direct influence on *H. capsulatum* numbers in culture alone either (data not shown), the intravacuolar situation has to create a different situation where glycolysis becomes essential. From these experiments, it cannot be with certainty deducted, if the abrogation of host cell- or fungal glycolysis is the detrimental factor. However, taking into account the results obtained by Friedrich (Friedrich 2016), intravacuolar *H. capsulatum* appears to be metabolically inactive compared to free *H. capsulatum.* Hence, reliance seems to be on the host glycolysis. Whether this provides an essential by-product or direct energy in the form of ATP needs to be elucidated.

Since *H. capsulatum* takes advantage of the increased glycolytic activity during infection, inhibition of glycolysis may be an interesting field to investigate pharmacologically. Having had an unsuccessful past in tumor therapy (Raez et al. 2013), 2-DG may have its renaissance in the field of anti-infectives.

4.5 Conclusion

The propounded thesis firstly elicits the extent and mode of HIF-1α regulation, the associated changes in inflammatory and metabolic gene expression, as well as the alterations induced by further chemical manipulation of HIF-1α during *H. capsulatum* infection in alveolar MΦ. It shows an active regulation of HIF-1α on a transcriptional and post-transcriptional level and a higher expression of the inflammatory and glycolytic HIF-1α target genes. Further, it shows that expression of human glycolytic genes is strongly driven by HIF-1α stabilizers and that higher expression levels of IL-1β can be achieved by HIF-1α stabilizers in murine, but not in human alveolar MΦ. Secondly, it characterizes the changes in metabolism during infection with regard to HIF-1α dependency. Both glycolysis and OXPHOS turnover were increased during infection. Herein, glycolysis did not depend on HIF-1α. Finally, the thesis elucidates the consequence of HIF-1α stabilizers and a glycolysis inhibitor for the outcome of infection, quantified by pathogen survival. While hypoxia, as it occurs in the *in vivo* infection, limited the survival of *H. capsulatum*, the use of chemical HIF-1α stabilizers did not result in altered *H. capsulatum* survival. Inhibition of glycolysis caused a considerable decline in the survival of *H. capsulatum,* opening the door for experiments with glycolysis inhibitors as anti-infective treatment options. Using alveolar MΦ, the experimental design created a simple mode of resembling the situation at the primary infection site during the early infection phase.

4.6 Outlook

This thesis elucidates the interaction of alveolar MΦ and *H. capsulatum* with regard to HIF-1α, its target genes and host cell metabolism. Looking on a broader scale it contributes to the research group's pursuit of firstly understanding and characterizing the physiological infection course on a cellular level to secondly deduct intervention strategies to combat *H. capsulatum* infection.

For an even better understanding of the physiological course of infection, it may help to resemble the situation at the infection site most closely. Herein, it is important to note that the phenotype of the alveolar MΦ *in vivo* is not necessarily the same as *in vitro.* Because alveolar MΦ inside the lungs are in a rather anti-inflammatory state, one could sort the M1 from the M2 cells or drive the seeded cells into either phenotype. Moreover, *in vivo* MΦ are not only found as single cells but also as multinucleated giant cells, which have been attributed with a higher capacity of destroying intracellular microbes (Lay et al. 2007, Gupta et al. 2010). This different conformation state of MΦ may strengthen HIF-1α's role in mediating the infection outcome.

Further, HIF-1α's role in the metabolic profile has not been fully investigated yet. While absence of HIF-1α did not alter the parameters of glycolysis, affection of OXPHOS by a HIF-1α knock-out has not been investigated in alveolar MΦ. Because OXPHOS was significantly higher during infection, it may be a host-protective or a pathogen-protective factor. Either way, its manipulation could potentially turn out to be a therapeutic working point to limit pathogen survival in the host cells. Generally, metabolic assay experiments were performed in murine cells, due to laboratory specific restrictions. Even though relevant preconditions were evaluated to be equal in mouse and human, experiments with human alveolar MΦ would bring more certainty for applying results to the human system.

Expanding hypoxia experiments beyond the role of HIF-1α may help to comprehend why MΦ get the edge on *H. capsulatum.* Herein, elevation of pro-inflammatory cytokines TNF-α or IFN-γ may play a decisive role (Schaible et al. 2010). Finally, further investigating the role of NF-κB in the transcriptional *hif1a* induction can potentially provide another working point for therapeutic intervention. For this purpose, displaying a cytosolic to nuclear shift of RelA/p65 and c-Rel, both subunits of NF-κB, is an experimentally established method (Isomura et al. 2009).

In terms of existing intervention strategies, analyzing the metabolic effects of HIF-1α stabilizers IOX2 or DMOG in metabolic assays for functional glycolysis and OXPHOS can help to understand why alveolar MΦ, as opposed to MDMΦ or BMDMΦ, were unable to degrade *H. capsulatum* when treated with those HIF-1α stabilizers. The importance of glycolysis in controlling and eventually degrading the pathogen is shown by the significant *H. capsulatum* reduction in 2-DG treated alveolar MΦ. Hence,

assessing the antifungal potential of further glycolysis inhibitors is of great interest, too. Herein, 3-bromopyruvate is an interesting approach, since research on its role in cancer therapy has been going on for years and thereby delivers a certain expertise in animal models already (Ganapathy-Kanniappan et al. 2010). To further investigate the role of glycolysis in the creation of a survival niche for *H. capsulatum*, it is crucial to find the metabolic intermediate which *H. capsulatum* utilizes for its energetic needs. Step-by-step inhibition of glycolysis and supplementation of glycolytic intermediates may help to identify this intermediate. With *in vitro* results being this promising, *in vivo* experiments with glycolysis inhibitors are the next step and preliminary experiments have started already.

5. Zusammenfassung

5.1 Einleitung

Der dimorphe Pilz *Histoplasma capsulatum* (*H. capsulatum*) ist Auslöser der Histoplasmose. Diese verläuft bei Patienten mit intaktem Immunsystem zumeist asymptomatisch oder als unkomplizierter grippaler Infekt. Immunschwache Patienten hingegen neigen zu schweren Verläufen mit systemischer Ausbreitung und zum Teil sogar tödlichem Ausgang. Im Gegensatz zu vielen anderen mikrobiellen Erregern erfolgt die Infektion nicht von Mensch zu Mensch, sondern durch in der Umwelt vorhandene Sporen. Diese finden sich in endemischen Regionen im Erdreich und vor allem in Vogelkot. Aufwirbeln der Sporen und anschließende Inhalation führen zur pulmonalen Infektion. Nach Aufnahme über die Lunge ändert *H. capsulatum* temperaturabhängig seine Konformation von Sporen und Hyphen in die sogenannte Hefeform. Alveolarmakrophagen (Alveolar-MΦ), die die gewebsspezifische lokale Makrophagen- (MΦ-) Population darstellen, phagozytieren *H. capsulatum.* Die Interaktionen von Wirt und Pathogen erzeugt eine Nische, die das Überleben von *H. capsulatum* in MΦ sichert. Zum entstehenden Mikromilieu gehören unter anderem durch Granulombildung verursachte Hypoxie, Aktivierung von Zellstoffwechsel und inflammatorische Zytokinausschüttung. In einem Modell mit aus Monozyten differenzierten MΦ (MDMΦ) wurde dabei gezeigt, dass die Infektion mit *H. capsulatum* zur Erhöhung des Hypoxie-induzierten Faktors-1α (HIF-1α) führt, worunter die intrazellulären Histoplasmen jedoch persistierten. Eine zusätzliche chemische HIF-1α Stabilisierung führte zur zellulären Aktivierung der MDMΦ und zum Abtöten der intrazellulären Histoplasmen ohne weitere Aktivierung des adaptiven Immunsystems.

In der hier vorgelegten Arbeit wurde die Bedeutung von HIF-1α für den Verlauf einer *H. capsulatum* Infektion in gewebsspezifischen Alveolar-MΦ untersucht. Unter der Hypothese, dass durch chemische HIF-1α Erhöhung Alveolar-MΦ die intrazellulären Histoplasmen abtöten können, wurden die Veränderung der HIF-1α Level während einer *H. capsulatum* Infektion dargestellt, die pro-inflammatorische und metabolische Zellantwort auf transkriptioneller und der Metabolismus zusätzlich auf funktioneller Ebene untersucht und zuletzt die Einflussnahme von Hypoxie, HIF-1α Stabilisatoren und einem Glykolyseinhibitor auf das Überleben von Histoplasmen in Alveolar-MΦ analysiert.

5.2 Material und Methoden

Methodische Grundlage der Experimente waren Alveolar-MΦ in Zellkultur. Humane Alveolar-MΦ wurden aus bronchoalveolären Lavagen (BAL) von Patienten gewonnen, murine Alveolar-MΦ wurden aus BAL von C57BL/6 Mäusen, beziehungsweise der entsprechenden HIF-1$\alpha^{-/-}$ Linie gewonnen. Die zur Infektion verwendeten Hefen der Linie *H. capsulatum* G217B wurden in Flüssigkultur bis zum Erreichen

der exponentiellen Wachstumsphase inkubiert. Die Infektionsrate betrug fünf Hefen pro MΦ (MOI 5:1). Bestimmung der intrazellulären Infektionslast erfolgte durch Lysieren der Alveolar-MΦ mit destilliertem H_2O und anschließender Inkubation des Lysats auf Agarplatten. Zur Quantifizierung von Proteinen wurde Western Blot, zur Quantifizierung von Messenger RNA (mRNA) quantitative Echtzeit-PCR (qRT-PCR) angewendet. Die Bestimmung des Zellmetabolismus erfolgte durch Analyse des Sauerstoffverbrauchs und des extrazellulären pH. Visuell wurde die Infektion durch Immunfluoreszenz- und Elektronenmikroskopie dargestellt.

5.3 Ergebnisse

Alveolar-MΦ zeigten unter Infektion mit *H. capsulatum* erhöhte HIF-1α Proteinlevel und eine vermehrte Expression des *hif1a* Gens. Fluoreszenzmikroskopisch zeigte sich in infizierten Alveolar-MΦ eine vermehrte HIF-1α Proteinanreicherung im Zellkern. Durch Hypoxie und den chemischen HIF-1α Stabilisator DMOG konnte ebenfalls eine Erhöhung des HIF-1α Proteinlevels gezeigt werden, die in beiden Fällen durch eine gleichzeitige Infektion keine weitere signifikante Steigerung zeigte. In murinen Alveolar-MΦ fand sich unter Infektion ebenfalls eine Erhöhung des HIF-1α Proteinlevels, sowie eine konstante, das Signifikanzniveau jedoch knapp verfehlende, Vermehrung der mRNA.

Der Aktivierungszustand von Alveolar-MΦ wurde anhand von metabolischer Aktivität und Genexpression sowie anhand der Genexpression pro-inflammatorischer Zytokine untersucht. Die Expression der glykolyseassoziierten und typischer Weise HIF-1α regulierten Gene GLUT-1 und PDK1 zeigte sich unter *H. capsulatum* Infektion vermehrt. Auch die chemische Stabilisierung von HIF-1α führte zu einer signifikanten GLUT-1- und PDK1-Mehrexpression, die durch gleichzeitige Infektion nicht weiter gesteigert werden konnte. Auch die Genexpression der pro-inflammatorischen Zytokine IL-1β und TNF-α ließ sich durch die Infektion mit *H. capsulatum* erhöhen. Für IL-1β wurden die Effekte einer chemischen HIF-1α Stabilisierung untersucht. Im Vergleich zur Infektion allein ließ sich die Expression des IL-1β Gens nur im murinen, nicht aber im humanen Modell durch zusätzliche chemische HIF-1α Stabilisierung während der Infektion steigern. In Experimenten zur oxidativen Phosphorylierung (OXPHOS) und der Glykolyse waren beide Stoffwechselwege der infizierten Alveolar-MΦ aktiver als die der Kontrollzellen. Ein Unterschied zwischen HIF-1α$^{-/-}$ Alveolar-MΦ und Wildtyp Alveolar-MΦ hinsichtlich der glykolytischen Aktivierung zeigte sich nicht.

Auf obige Experimente aufbauend wurden Hypoxie, chemische HIF-1α Stabilisierung und Inhibition der Glykolyse als mögliche Einflussfaktoren auf das intrazelluläre Überleben von Histoplasmen untersucht. Hierbei zeigte sich unter Hypoxie eine um 53± 20% geringere Erregerlast gegenüber der Infektion unter normoxischen Bedingungen. Durch chemische HIF-1α Stabilisierung ließ sich jedoch keine Reduktion des Wachstums von Histoplasmen erzielen. Um den Einfluss der Glykolyse auf das intrazelluläre

Überleben von Histoplasmen zu untersuchen, wurde mit 2-Deoxy-Glucose (2-DG) die Hexokinase gehemmt. Hierunter zeigte sich eine dosisabhängige Reduktion des intrazellulären Wachstums von Histoplasmen. Die Untersuchung der Überstände konnte einen artifiziellen Effekt durch Einschränkung der Phagozytose oder vermehrte Freisetzung von *H. capsulatum* ausschließen. In der Elektronenmikroskopie wurde die Zersetzung der phagozytierten intrazellulären Histoplasmen in mit 2-DG behandelten Alveolar-MΦ dargestellt.

5.4 Diskussion

Die Erkenntnisse zur Bedeutung von HIF-1α haben sich in den vergangenen Jahren vom Verständnis als klassischem Regulator der Zellhomöostase unter Hypoxie weit auf die Bereiche Inflammation und Infektion ausgedehnt. In Modellen mit *Candida albicans* und *Aspergillus fumigatus* wie auch für *H. capsulatum* konnte gezeigt werden, dass HIF-1α defiziente Mäuse höhere Erregerlasten und Mortalität zeigen als HIF-1α kompetente Mäuse. Darüber hinaus konnte unsere Arbeitsgruppe im Modell mit MDMΦ zeigen, dass die zusätzliche pharmakologische HIF-1α Erhöhung eine mögliche Therapieoption zur Erregerlastreduktion darstellt. Diese Thesis stellt nun die Bedeutung von HIF-1α für die am primären Infektionsort vorhandenen Alveolar-MΦ in den Fokus.

Die HIF-1α Regulation in Alveolar-MΦ scheint den gleichen Prinzipien zu folgen, wie sie bereits in anderen MΦ Populationen erforscht wurden. So stellen sowohl die Infektion mit *H. capsulatum* als auch HIF-1α Stabilisatoren und Hypoxie adäquate Stimulatoren zur HIF-1α Erhöhung dar. Auf transkriptioneller Ebene scheint unter Infektion vor allem NF-κB, ein bekannter Induktor des *hif1a* Gens, von Bedeutung zu sein. Dies legen die IL-1β und TNF-α Erhöhungen nahe, denn beide Zytokine sind beschriebene Induktoren von NF-κB. Spezifisch für *H. capsulatum* sind Dectin-1 und Komplementrezeptor (CR) 3 über Syk und das *H. capsulatum* Oberflächenprotein Yps3p über den toll-like Rezeptor (TLR) 2 an der NF-κB Aktivierung beteiligt. Experimente, die erhöhte NF-κB Level oder eine nukleare Translokation durch eine *H. capsulatum* Infektion beweisen, fehlen jedoch aktuell. Sollte sich NF-κB als HIF-1α-Induktor bei *H. capsulatum* bestätigen, würde dies einen weiteren Ansatzpunkt für die experimentelle HIF-1α Manipulation darstellen. Auf post-transkriptioneller Ebene spielen klassischer Weise ein erhöhter Sauerstoffverbrauch durch die Infektion, sowie das Anfallen der Metabolite Succinat und Laktat eine Rolle. Beides führt zu einer Hemmung von Prolyl-Hydroxylasen und somit zu vermindertem HIF-1α Abbau. Die vermehrte Glykolyse und gesteigerte OXPHOS der infizierten Alveolar-MΦ sprechen für ein vermehrtes Anfallen von Succinat und Laktat.

Eng mit HIF-1α verknüpft ist der Metabolismus der Wirtszelle. Er gibt allgemein Hinweise auf ihren Aktivierungszustand. So ist eine gesteigerte Glykolyse bei MΦ mit einem pro-inflammatorischen Phänotyp assoziiert. Bei anderen intrazellulären Erregern wie *Chlamydia trachomatis* oder

Mycobacterium tuberculosis wird typischerweise eine solche Aktivierung der Wirtsglykolyse beschrieben, die dort zur Reduktion der Erregerlast beiträgt. Diese Glykolyseaktivierung wird am ehesten über TLR-Signalwege und bei Pilzinfektionen durch die von β-Glucan angestoßene Dectin-1 – Akt – mTOR – HIF-1α Kaskade gesteuert. Zwar zeigten Alveolar-MΦ durch die Infektion mit *H. capsulatum* eine erhöhte Glykolyseaktivität, entgegen den Erwartungen zeigten HIF-1α$^{-/-}$ Alveolar-MΦ jedoch keine Einschränkungen in ihrer glykolytischen Aktivität. Folglich scheint die Aktivierung der Glykolyse bei Alveolar-MΦ unter *H. capsulatum* Infektion auf HIF-1α unabhängigem Wege, zum Beispiel über TLR2 oder TNF-α, möglich zu sein. Interessanterweise zeigte sich auch eine Aktivierung der oxidativen Phosphorylierung (OXPHOS). In der Regel wird der Metabolismus infizierter Immunzellen als Wechsel von OXPHOS hin zur Glykolyse, ähnlich dem Warburg-Effekt, beschrieben. Auch die vermehrte Expression von PDK1, einem Enzym, das die Bereitstellung von Acetyl-CoA für die OXPHOS limitiert, hätte dies vermuten lassen. Somit liegt die Schlussfolgerung nahe, dass neben Acetyl-CoA andere Metabolite wie Glutamin in den Zitratzyklus eingeschleust werden und eine solche Aktivierung ermöglichen. Glutamin ist eine der mengenmäßig häufigsten Aminosäuren und konnte bereits als entscheidender Energieträger zur ATP-Gewinnung in MΦ identifiziert werden.

In den obigen Beschreibungen der Anpassungsmechanismen der Alveolar-MΦ unter Infektion liegt schlussendlich das Ziel, eine Interventionsmöglichkeit zu finden das intrazelluläre Überleben von *H. capsulatum* zu verhindern. Hierbei konnte unsere Arbeitsgruppe in Experimenten mit MDMΦ bereits zeigen, dass eine chemische Stabilisierung von HIF-1α über das physiologische Maß hinaus die intrazelluläre Erregerlast verringern und somit einen möglichen Therapieansatz darstellen kann. Dass sich dieser Effekt in Alveolar-MΦ nicht bestätigte, könnte darin begründet sein, dass sie im Alveolarraum mit einer Vielzahl an fremden Antigenen in Kontakt kommen und dort die Aufgabe haben eine Balance zwischen Pro- und Anti-Inflammation aufrechtzuerhalten. Es liegt daher nahe, dass ihr Potenzial für eine ausgeprägte pro-inflammatorische Antwort geringer ist als das von MDMΦ. Passend dazu ließ sich durch chemische HIF-1α Stabilisierung während der Infektion nur bedingt die Expression des pro-inflammatorischen IL-1β steigern. Verglichen mit dem Wissen über die Bedeutung des HIF-1α Signalwegs für die Immunabwehr, ist die Rolle der metabolischen Anpassungen und die Möglichkeiten der Nutzung von Glykolyseinhibitoren als Antiinfektiva wesentlich weniger erforscht. Die hier gezeigte Reduktion der Erregerlast unter dem Hexokinase-Inhibitor 2-DG legt nahe, dass die intrazellulären Histoplasmen während der Infektion von der Wirtsglykolyse abhängig sind. Eine Differenzierung welche Glykolysemetabolite für das intrazelluläre Überleben von *H. capsulatum* entscheidend sind fehlt aktuell, würde aber sicherlich eine gezieltere Erforschung von Glykolyseinhibitoren als Antiinfektiva erlauben.

6. References

6.1 Journal publications

Abu Kwaik Y and Bumann D. (2015). "Host Delivery of Favorite Meals for Intracellular Pathogens." *PLoS Pathogens* 11: 1–8.

Acosta-Iborra B, Elorza A, Olazabal IM, Martín-Cofreces NB, Martin-Puig S, Miró M, Calzada MJ, Aragonés J, Sánchez-Madrid F and Landázuri MO. (2009). "Macrophage Oxygen Sensing Modulates Antigen Presentation and Phagocytic Functions Involving IFN-γ Production through the HIF-1α Transcription Factor." *The Journal of Immunology* 182: 3155-3164.

Anand RJ, Gribar SC, Li J, Kohler JW, Branca MF, Dubowski T, Sodhi CP and Hackam DJ. (2007). "Hypoxia Causes an Increase in Phagocytosis by Macrophages in a HIF-1α-dependent Manner." *Journal of Leukocyte Biology* 82: 1257–1265.

Antinori S. (2014). "*Histoplasma Capsulatum*: More Widespread than Previously Thought." *The American Journal of Tropical Medicine and Hygiene* 90: 982–983.

Aravalli RN, Hu S, Woods JP and Lokensgard JR. (2008). "*Histoplasma Capsulatum* Yeast Phase-Specific Protein Yps3p Induces Toll-like Receptor 2 Signaling." *Journal of Neuroinflammation* 5: 30.

Arnheim J and Rosenbaum A. (1904). "Ein Beitrag Zur Frage Der Zuckerzerstörung Im Tierkörper Durch Fermentwirkung (Glykolyse)." *Hoppe-Seyler´ s Zeitschrift Für Physiologische Chemie* 40: 220–233.

Ashbee HR, Evans EG V, Viviani MA, Dupont B, Chryssanthou E, Surmont I, Tomsikova A, Vachkov P, Ener B, Zala J and Tintelnot K. (2008). "Histoplasmosis in Europe: Report on an Epidemiological Survey from the European Confederation of Medical Mycology Working Group." *Medical Mycology* 46: 57–65.

Beck-Schimmer B, Schimmer RC, Madjdpour C, Bonvini JM, Pasch T and Ward PA. (2001). "Hypoxia Mediates Increased Neutrophil and Macrophage Adhesiveness to Alveolar Epithelial Cells." *American Journal of Respiratory Cell and Molecular Biology* 25: 780–787.

Berra E, Benizri E, Ginouvès A, Volmat V, Roux D and Pouysségur J. (2003). "HIF Prolyl-hydroxylase 2 Is the Key Oxygen Sensor Setting Low Steady-state Levels of HIF-1α in Normoxia." *The EMBO Journal* 22: 4082–4090.

Bhandari T and Nizet V. (2014). "Hypoxia-Inducible Factor (HIF) as a Pharmacological Target for Prevention and Treatment of Infectious Diseases." *Infectious Diseases and Therapy* 3: 159–174.

Bowden SD, Rowley G, Hinton JCD and Thompson A. (2009). "Glucose and Glycolysis Are Required for the Successful Infection of Macrophages and Mice by *Salmonella Enterica* Serovar Typhimurium." *Infection and Immunity* 77: 3117–3126.

Brummer E and Stevens DA. (1995). "Antifungal Mechanisms of Activated Murine Bronchoalveolar or Peritoneal Macrophages for *Histoplasma Capsulatum*." *Clinical & Experimental Immunology* 102: 65–70.

Carreau A, Hafny-Rahbi El B, Matejuk A, Grillon C and Kieda C. (2011). "Why Is the Partial Oxygen Pressure of Human Tissues a Crucial Parameter? Small Molecules and Hypoxia." *Journal of Cellular and Molecular Medicine* 15: 1239–1253.

Cartee T V, White KJ, Newton-West M and Swerlick RA. (2012). “Hypoxia and Hypoxia Mimetics Inhibit TNF-Dependent VCAM1 Induction in the 5A32 Endothelial Cell Line via a Hypoxia Inducible Factor Dependent Mechanism.” *Journal of Dermatological Science* 65: 86–94.

Chan MC, Ilott NE, Schödel J, Sims D, Tumber A, Lippl K, Mole DR, Pugh CW, Ratcliffe PJ, Ponting CP and Schofield CJ. (2016). “Tuning the Transcriptional Response to Hypoxia by Inhibiting Hypoxia-Inducible Factor (HIF) Prolyl and Asparaginyl Hydroxylases.” *Journal of Biological Chemistry* 291: 20661–20673.

Chen C, Pore N, Behrooz A, Ismail-Beigi F and Maity A. (2001). “Regulation of Glut1 MRNA by Hypoxia-Inducible Factor-1: INTERACTION BETWEEN H-Ras AND HYPOXIA.” *Journal of Biological Chemistry* 276: 9519–9525.

Cheng S-C, Quintin J, Cramer RA, Shepardson KM, Saeed S, Kumar V, Giamarellos-Bourboulis EJ, Martens JHA, Rao NA, Aghajanirefah A, Manjeri GR, Li Y, Ifrim DC, Arts RJW, Veer BMJW van der, Deen PMT, Logie C, O’Neill LA, Willems P, Veerdonk FL van de, Meer JWM van der, Ng A, Joosten LAB, Wijmenga C, Stunnenberg HG, Xavier RJ and Netea MG. (2014). “MTOR- and HIF-1α–mediated Aerobic Glycolysis as Metabolic Basis for Trained Immunity.” *Science* 345: 1250684.

Chowdhury R, Candela-lena JI, Chan MC, Greenald DJ, Yeoh KK, Tian Y, Mcdonough MA, Tumber A, Rose NR, Conejo-garcia A, Demetriades M, Mathavan S, Kawamura A, Lee MK and Eeden F Van. (2013). “Selective Small Molecule Probes for the Hypoxia Inducible Factor (HIF) Prolyl Hydroxylases.” *ACS Chemical Biology* 8: 2–10.

Covarrubias AJ, Aksoylar HI and Horng T. (2015). “Control of Macrophage Metabolism and Activation by MTOR and Akt Signaling.” *Seminars in Immunology* 27: 286–296.

Cramer T, Yamanishi Y, Clausen BE, Förster I, Pawlinski R, Mackman N, Haase VH, Jaenisch R, Corr M, Nizet V, Firestein GS, Gerber HP, Ferrara N and Johnson RS. (2003). “HIF-1α Is Essential for Myeloid Cell-Mediated Inflammation.” *Cell* 112: 645–657.

Czyz DM, Willett JW and Crosson S. (2017). “*Brucella Abortus* Induces a Warburg Shift in Host Metabolism That Is Linked to Enhanced Intracellular Survival of the Pathogen.” *Journal of Bacteriology* 199: 1–14.

Darling S. (1906). “A Protozoön General Infection Producing Pseudotubercles in the Lungs and Focal Necroses in the Liver, Spleen and Lymphnodes.” *Journal of the American Medical Association* XLVI: 1283–1285.

Davies LC, Jenkins SJ, Allen JE and Taylor PR. (2013). “Tissue-Resident Macrophages.” *Nature Immunology* 14: 986–995.

Deepe GS. (2000). “Immune Response to Early and Late *Histoplasma Capsulatum* Infections.” *Current Opinion in Microbiology* 3: 359–362.

Deepe GS, Gibbons R and Woodward E. (1999). “Neutralization of Endogenous Granulocyte-Macrophage Colony-Stimulating Factor Subverts the Protective Immune Response to *Histoplasma Capuslatum*.” *The Journal of Immunology* 163: 4985–4993.

Deppe J, Popp T, Egea V, Steinritz D, Schmidt A, Thiermann H, Weber C and Ries C. (2016). “Impairment of Hypoxia-Induced HIF-1α Signaling in Keratinocytes and Fibroblasts by Sulfur Mustard Is Counteracted by a Selective PHD-2 Inhibitor.” *Archives of Toxicology* 90: 1141–1150.

Drecktrah D, Knodler LA, Howe D and Steele-Mortimer O. (2007). "*Salmonella* Trafficking Is Defined by Continuous Dynamic Interactions with the Endolysosomal System." *Traffic* 8: 212–225.

DuBois JC, Pasula R, Dade JE and Smulian AG. (2016). "Yeast Transcriptome and In Vivo Hypoxia Detection Reveals *Histoplasma Capsulatum* Response to Low Oxygen Tension." *Medical Mycology* 54: 40–58.

DuBois JC and Smulian AG. (2016). "Sterol Regulatory Element Binding Protein (Srb1) Is Required for Hypoxic Adaptation and Virulence in the Dimorphic Fungus *Histoplasma Capsulatum*." *PLOS ONE* 11: e0163849.

Eltzschig HK and Carmeliet P. (2011). "Hypoxia and Inflammation." *New England Journal of Medicine* 364: 656–665.

Fan D, Coughlin LA, Neubauer MM, Kim J, Kim MS, Zhan X, Simms-Waldrip TR, Xie Y, Hooper L V and Koh AY. (2015). "Activation of HIF-1α and LL-37 by Commensal Bacteria Inhibits *Candida Albicans* Colonization." *Nature Medicine* 21: 808–814.

Fangradt M, Hahne M, Gaber T, Strehl C, Rauch R, Hoff P, Löhning M, Burmester G-R and Buttgereit F. (2012). "Human Monocytes and Macrophages Differ in Their Mechanisms of Adaptation to Hypoxia." *Arthritis Research & Therapy* 14: R181.

Fecher RA, Horwath MC, Friedrich D, Rupp J and Deepe GS. (2016). "Inverse Correlation between IL-10 and HIF-1α in Macrophages Infected with *Histoplasma Capsulatum*." *The Journal of Immunology* 197: 565–579.

Fels AO and Cohn ZA. (1986). "The Alveolar Macrophage." *Journal of Applied Physiology* 60: 353–369.

Friedrich D, Fecher RA, Rupp J and Deepe GS. (2017). "Impact of HIF-1α and Hypoxia on Fungal Growth Characteristics and Fungal Immunity." *Microbes and Infection* 19: 204–209.

Galván-Peña S and O'Neill LAJ. (2014). "Metabolic Reprograming in Macrophage Polarization." *Frontiers in Immunology* 5: 420.

Ganapathy-Kanniappan, Vali M, Kunjithapatham R, Buijs M, Syed LH, Rao PP, Ota S, Kwak BK, Loffroy R and Geschwind J-F. (2010). "Anticancer Efficacy of the Metabolic Blocker 3-Bromopyruvate : Specific Molecular 3-Bromopyruvate : A New Targeted Antiglycolytic Agent and a Promise for Cancer Therapy." *Current Pharmaceutical Biotechnology* 11: 510–517.

Garfoot AL and Rappleye CA. (2016). "Histoplasma Capsulatum Surmounts Obstacles to Intracellular Pathogenesis." *FEBS Journal* 283: 619–633.

Gatenby RA and Gillies RJ. (2004). "Why Do Cancers Have High Aerobic Glycolysis?" *Nature Reviews Cancer* 4: 891–899.

Giaccia A, Siim BG and Johnson RS. (2003). "HIF-1 as a Target for Drug Development." *Nature Reviews Drug Discovery* 2 (October): 803–811.

Gildea LA, Morris RE and Newman SL. (2001). "*Histoplasma Capsulatum* Yeasts Are Phagocytosed Via Very Late Antigen-5, Killed, and Processed for Antigen Presentation by Human Dendritic Cells." *The Journal of Immunology* 166: 1049–1056.

Gleeson LE, Sheedy FJ, Palsson-McDermott EM, Triglia D, O'Leary SM, O'Sullivan MP, O'Neill LAJ and Keane J. (2016). "Cutting Edge: *Mycobacterium Tuberculosis* Induces Aerobic Glycolysis in Human Alveolar Macrophages That Is Required for Control of Intracellular Bacillary Replication." *The Journal of Immunology* 196: 2444–2449.

Gomez FJ, Pilcher-Roberts R, Alborzi A and Newman SL. (2008). "*Histoplasma Capsulatum* Cyclophilin A Mediates Attachment to Dendritic Cell VLA-5." *The Journal of Immunology* 181: 7106–7114.

Gonzalez NC, Allen J, Blanco VG, Schmidt EJ, Rooijen N van and Wood JG. (2007). "Alveolar Macrophages Are Necessary for the Systemic Inflammation of Acute Alveolar Hypoxia." *Journal of Applied Physiology* 103: 1386–1394.

Gottfried E, Kreutz M and Mackensen A. (2012). "Tumor Metabolism as Modulator of Immune Response and Tumor Progression." *Seminars in Cancer Biology* 22: 335–341.

Grahl N, Shepardson KM, Chung D and Cramer RA. (2012). "Hypoxia and Fungal Pathogenesis: To Air or Not To Air?" *Eukaryotic Cell* 11: 560–570.

Guimarães AJ, Cerqueira MD de and Nosanchuk JD. (2011). "Surface Architecture of *Histoplasma Capsulatum*." *Frontiers in Microbiology* 2: 1–14.

Gupta N, Arora SK, Rajwanshi A, Nijhawan R and Srinivasan R. (2010). "Histoplasmosis : Cytodiagnosis and Review of Literature with Special Emphasis on Differential Diagnosis on Cytomorphology." *Cytopathology* 21: 240–244.

Hartmann H, Eltzschig HK, Wurz H, Hantke K, Rakin A, Yazdi AS, Matteoli G, Bohn E, Autenrieth IB, Karhausen J, Neumann D, Colgan SP and Kempf VAJ. (2018). "Hypoxia-Independent Activation of HIF-1 by Enterobacteriaceae and Their Siderophores." *Gastroenterology* 134: 756–767.

Heiden MG Vander, Cantley LC and Thompson CB. (2009). "Understanding the Warburg Effect: The Metabolic Requirements of Cell Proliferation." *Science* 324: 1029–1033.

Hellwig-Bürgel T, Stiehl DP, Wagner AE, Metzen E and Jelkmann W. (2005). "*Review:* Hypoxia-Inducible Factor-1 (HIF-1): A Novel Transcription Factor in Immune Reactions." *Journal of Interferon & Cytokine Research* 25: 297–310.

Hempel SL, Monick MM and Hunninghake GW. (1996). "Effect of Hypoxia on Release of IL-1 and TNF by Human Alveolar Macrophages." *American Journal of Respiratory Cell and Molecular Biology* 14: 170–176.

Heninger E, Hogan LH, Karman J, Macvilay S, Hill B, Woods JP and Sandor M. (2006). "Characterization of the *Histoplasma Capsulatum*-Induced Granuloma." *The Journal of Immunology* 177: 3303 LP-3313.

Hilty J, George Smulian A and Newman SL. (2011). "*Histoplasma Capsulatum* Utilizes Siderophores for Intracellular Iron Acquisition in Macrophages." *Medical Mycology* 49: 633–642.

Hoesel B and Schmid JA. (2013). "The Complexity of NF-KB Signaling in Inflammation and Cancer." *Molecular Cancer* 12: 86.

Horwath MC, Fecher RA and Deepe G. (2016). "*Histoplasma Capsulatum*, Lung Infection and Immunity." *Future Microbiology*, 10: 967–975.

Hussell T and Bell TJ. (2014). "Alveolar Macrophages: Plasticity in a Tissue-Specific Context." *Nature Reviews Immunology* 14: 81–93.

Hwang LH, Mayfield JA, Rine J and Sil A. (2008). "*Histoplasma* Requires SID1, a Member of an Iron-Regulated Siderophore Gene Cluster, for Host Colonization." *PLoS Pathogens* 4: e1000044.

Ishii H, Hayashi S, Hogg JC, Fujii T, Goto Y, Sakamoto N, Mukae H, Vincent R and Eeden SF van. (2005). "Alveolar Macrophage-Epithelial Cell Interaction Following Exposure to Atmospheric Particles Induces the Release of Mediators Involved in Monocyte Mobilization and Recruitment." *Respiratory Research* 6: 87.

Isomura I, Palmer S, Grumont RJ, Bunting K, Hoyne G, Wilkinson N, Banerjee A, Proietto A, Gugasyan R, Wu L, McNally A, Steptoe RJ, Thomas R, Shannon MF and Gerondakis S. (2009). "C-Rel Is Required for the Development of Thymic Foxp3 $^{+}$ CD4 Regulatory T Cells." *The Journal of Experimental Medicine* 206: 3001–3014.

Iyer N V, Kotch LE, Agani F, Leung SW, Laughner E, Wenger RH, Gassmann M, Gearhart JD, Lawler AM, Yu AY and Semenza GL. (1998). "Cellular and Developmental Control of O2 Homeostasis by Hypoxia-Inducible Factor 1α." *Genes & Development* 12: 149–162.

Jaakkola P, Jaakkola P, Mole DR, Tian Y, Kriegsheim A Von, Hebestreit HF, Mukherji M, Schofield CJ and Ratcliffe PJ. (2001). "Targeting of HIF-a to the von Hippel – Lindau Ubiquitylation Complex by O 2 -Regulated Prolyl Hydroxylation." *Science* 292: 468–472.

Jr-Shiuan L, Juin-Hua H, Li-Yin H, Sheng-Yang W and Wu-Hsieh B. (2010). "Distinct Roles of Complement Receptor 3, Dectin-1, and Sialic Acids in Murine Macrophage Interaction with *Histoplasma* Yeast." *Journal of Leukocyte Biology* 88: 95–106.

Kasuga T, White TJ, Koenig G, Mcewen J, Restrepo A, Castañeda E, Silva Lacaz C Da, Heins-Vaccari EM, Freitas RS De, Zancopé-Oliveira RM, Qin Z, Negroni R, Carter DA, Mikami Y, Tamura M, Taylor ML, Miller GF, Poonwan N and Taylor JW. (2003). "Phylogeography of the Fungal Pathogen *Histoplasma Capsulatum*." *Molecular Ecology* 12: 3383–3401.

Kauffman CA. (2007). "Histoplasmosis: A Clinical and Laboratory Update." *Clinical Microbiology Reviews* 20: 115–132.

Kauffman CA. (2017). "Treatment of the Midwestern Endemic Mycoses, Blastomycosis and Histoplasmosis." *Current Fungal Infection Reports* 11: 67–74.

Kelly B and O'Neill LAJ. (2015). "Metabolic Reprogramming in Macrophages and Dendritic Cells in Innate Immunity." *Cell Research* 25: 771–784.

Kim J, Tchernyshyov I, Semenza GL and Dang C V. (2006). "HIF-1-Mediated Expression of Pyruvate Dehydrogenase Kinase: A Metabolic Switch Required for Cellular Adaptation to Hypoxia." *Cell Metabolism* 3: 177–185.

Kirk K and Lehane AM. (2014). "Membrane Transport in the Malaria Parasite and Its Host Erythrocyte." *Biochemical Journal* 457: 1–18.

Kobayashi K, Kaneda K and Kasama T. (2001). "Immunopathogenesis of Delayed-Type Hypersensitivity." *Microscopy Research and Technique* 53: 241–245.

Koslowski M, Luxemburger U, Türeci Ö and Sahin U. (2010). "Tumor-Associated CpG Demethylation Augments Hypoxia-Induced Effects by Positive Autoregulation of HIF-1α." *Oncogene* 30: 876–882.

Krawczyk CM, Holowka T, Sun J, Blagih J, Amiel E, DeBerardinis RJ, Cross JR, Jung E, Thompson CB, Jones RG and Pearce EJ. (2010). "Toll-like Receptor–induced Changes in Glycolytic Metabolism Regulate Dendritic Cell Activation." *Blood* 115: 4742–4749.

Laemmli UK. (1970). "Cleavage of Structural Proteins during the Assembly of the Head of Bacteriophage T4." *Nature* 227: 680–685.

Lay G, Poquet Y, Puissegur M, Botanch C, Bon H, Levillain F, Duteyrat J and Emile J. (2007). "Langhans Giant Cells from *M . Tuberculosis* -Induced Human Granulomas Cannot Mediate Mycobacterial Uptake." *The Journal of Pathology* 211: 76–85.

Lee B-H and Ruoslahti E. (2005). "A5β1 Integrin Stimulates Bcl-2 Expression and Cell Survival through Akt, Focal Adhesion Kinase, and Ca2+/Calmodulin-Dependent Protein Kinase IV." *Journal of Cellular Biochemistry* 95: 1214–1223.

Lee J-W, Bae S-H, Jeong J-W, Kim S-H and Kim K-W. (2004). "Hypoxia-Inducible Factor (HIF-1)α: Its Protein Stability and Biological Functions." *Experimental & Molecular Medicine* 36: 1–12.

Long KH, Gomez FJ, Morris RE and Newman SL. (2003). "Identification of Heat Shock Protein 60 as the Ligand on *Histoplasma Capsulatum* That Mediates Binding to CD18 Receptors on Human Macrophages." *The Journal of Immunology* 170: 487–494.

Lu H, Forbes RA and Verma A. (2002). "Hypoxia-Inducible Factor 1 Activation by Aerobic Glycolysis Implicates the Warburg Effect in Carcinogenesis." *Journal of Biological Chemistry* 277: 23111–23115.

Maček I, Dumbrell AJ, Nelson M, Fitter AH, Vodnik D and Helgason T. (2011). "Local Adaptation to Soil Hypoxia Determines the Structure of an Arbuscular Mycorrhizal Fungal Community in Roots from Natural CO2 Springs ." *Applied and Environmental Microbiology* 77: 4770–4777.

Medoff G, Sacco M, Maresca B, Schlessinger D, Painter A, Kobayashi GS and Carratu L. (1986). "Irreversible Block of the Mycelial-to-Yeast Phase Transition of *Histoplasma Capsulatum*." *Science* 231: 476 LP-479.

Melillo G, Musso T, Sica A, Taylor LS, Cox GW and Varesio L. (1995). "A Hypoxia-Responsive Element Mediates a Novel Pathway of Activation of the Inducible Nitric Oxide Synthase Promoter." *The Journal of Experimental Medicine* 182: 1683–1693.

Mosser DM and Edwards JP. (2008). "Exploring the Full Spectrum of Macrophage Activation." *Nature Reviews Immunology* 8: 958–969.

Muraille E, Leo O and Moser M. (2014). "Th1/Th2 Paradigm Extended: Macrophage Polarization as an Unappreciated Pathogen-Driven Escape Mechanism?" *Frontiers in Immunology* 5: 1–12.

Murray PJ and Wynn TA. (2011). "Protective and Pathogenic Functions of Macrophage Subsets." *Nature Reviews Immunology* 11: 723–737.

Newman SL, Bucher C, Rhodes J and Bullock WE. (1990). "Phagocytosis of *Histoplasma Capsulatum* Yeasts and Microconidia by Human Cultured Macrophages and Alveolar Macrophages. Cellular Cytoskeleton Requirement for Attachment and Ingestion." *Journal of Clinical Investigation* 85: 223–230.

Newman SL, Gootee L, Morris R and Bullock WE. (1992). "Digestion of *Histoplasma Capsulatum* Yeasts by Human Macrophages." *The Journal of Immunology* 149: 574–580.

Newsholme P. (2001). “Why Is L-Glutamine Metabolism Important to Cells of the Immune System in Health, Postinjury, Surgery or Infection?” *The Journal of Nutrition* 131: 2515S–2522S.

Nizet V and Johnson RS. (2009). “Interdependence of Hypoxic and Innate Immune Responses.” *Nature Reviews Immunology* 9: 609–617.

Ojcius DM, Degani H, Mispelter J and Dautry-Varsat A. (1998). “Enhancement of ATP Levels and Glucose Metabolism during an Infection by Chlamydia : NMR STUDIES OF LIVING CELLS.” *Journal of Biological Chemistry* 273: 7052–7058.

Owen OE, Kalhan SC and Hanson RW. (2002). “The Key Role of Anaplerosis and Cataplerosis for Citric Acid Cycle Function.” *Journal of Biological Chemistry* 277: 30409–30412.

Pearce EL and Pearce EJ. (2013). “Metabolic Pathways in Immune Cell Activation and Quiescence.” *Immunity* 38: 633–643.

Pike Winer LS and Wu M. (2014). “Rapid Analysis of Glycolytic and Oxidative Substrate Flux of Cancer Cells in a Microplate.” *PLOS ONE* 9: e109916.

Raez LE, Papadopoulos K, Ricart AD, Chiorean EG, Dipaola RS, Stein MN, Rocha Lima CM, Schlesselman JJ, Tolba K, Langmuir VK, Kroll S, Jung DT, Kurtoglu M, Rosenblatt J and Lampidis TJ. (2013). “A Phase i Dose-Escalation Trial of 2-Deoxy-d-Glucose Alone or Combined with Docetaxel in Patients with Advanced Solid Tumors.” *Cancer Chemotherapy and Pharmacology* 71: 523–530.

Ray K, Marteyn B, Sansonetti PJ and Tang CM. (2009). “Life on the inside: The Intracellular Lifestyle of Cytosolic Bacteria.” *Nature Reviews Microbiology* 7: 333–340.

Rius J, Guma M, Schachtrup C, Akassoglou K, Zinkernagel AS, Nizet V, Johnson RS, Haddad GG and Karin M. (2008). “NF-KB Links Innate Immunity to the Hypoxic Response through Transcriptional Regulation of HIF-1α.” *Nature* 453: 807–811.

Rodríguez-Prados J-C, Través PG, Cuenca J, Rico D, Aragonés J, Martín-Sanz P, Cascante M and Boscá L. (2010). “Substrate Fate in Activated Macrophages: A Comparison between Innate, Classic, and Alternative Activation.” *The Journal of Immunology* 185: 605–614.

Rosenfeld E and Beauvoit B. (2003). “Role of the Non-Respiratory Pathways in the Utilization of Molecular Oxygen by *Saccharomyces Cerevisiae*.” *Yeast* 20: 1115–1144.

Rustad TR, Harrell MI, Liao R and Sherman DR. (2008). “The Enduring Hypoxic Response of *Mycobacterium Tuberculosis*.” *PLOS ONE* 3: e1502.

Sabroe I, Read RC, Whyte MKB, Dockrell DH, Vogel SN and Dower SK. (2003). “Toll-Like Receptors in Health and Disease: Complex Questions Remain.” *The Journal of Immunology* 171: 1630–1635.

Schaffer K and Taylor CT. (2015). “The Impact of Hypoxia on Bacterial Infection.” *FEBS Journal* 282: 2260–2266.

Schaible B, Schaffer K and Taylor CT. (2010). “Hypoxia, Innate Immunity and Infection in the Lung.” *Respiratory Physiology and Neurobiology* 174: 235–243.

Schertzer JD and Steinberg GR. (2014). “Immunometabolism: The Interface of Immune and Metabolic Responses in Disease.” *Immunology And Cell Biology* 92: 303.

Scholz CC and Taylor CT. (2013). “Targeting the HIF Pathway in Inflammation and Immunity.” *Current Opinion in Pharmacology* 13: 646–653.

Sebghati TS, Engle JT and Goldman WE. (2000). “Intracellular Parasitism by *Histoplasma Capsulatum*: Fungal Virulence and Calcium Dependence.” *Science* 290: 1368–1372.

Selak MA, Armour SM, MacKenzie ED, Boulahbel H, Watson DG, Mansfield KD, Pan Y, Simon MC, Thompson CB and Gottlieb E. (2005). “Succinate Links TCA Cycle Dysfunction to Oncogenesis by Inhibiting HIF-α Prolyl Hydroxylase.” *Cancer Cell* 7: 77–85.

Semenza GL. (2000). “HIF-1 and Human Disease: One Highly Involved Factor.” *Genes & Development* 14: 1983–1991.

Semenza GL, Nejfelt MK, Chi SM and Antonarakis SE. (1991). “Hypoxia-Inducible Nuclear Factors Bind to an Enhancer Element Located 3’ to the Human Erythropoietin Gene.” *Proceedings of the National Academy of Sciences of the United States of America* 88: 5680–5684.

Serasanambati M and Chilakapati SR. (2016). “Function of Nuclear Factor Kappa B (NF-KB) in Human Diseases-A Review.” *South Indian Journal of Biological Sciences* 2: 368–387.

Sever JL and Youmans GP. (1957). “The Relation of Oxygen Tension to Virulence of Tubercle Bacilli and to Acquired Resistance in Tuberculosis.” *The Journal of Infectious Diseases* 101: 193–202.

Shepardson KM, Jhingran A, Caffrey A, Obar JJ, Suratt BT, Berwin BL, Hohl TM and Cramer RA. (2014). “Myeloid Derived Hypoxia Inducible Factor 1-Alpha Is Required for Protection against Pulmonary *Aspergillus Fumigatus* Infection.” *PLOS Pathogens* 10: e1004378.

Simon LM, Robin ED, Phillips JR, Acevedo J, Axline SG and Theodore J. (1977). “Enzymatic Basis for Bioenergetic Differences of Alveolar versus Peritoneal Macrophages and Enzyme Regulation by Molecular O2.” *Journal of Clinical Investigation* 59: 443–448.

Sonveaux P, Copetti T, Saedeleer CJ De, Végran F, Verrax J, Kennedy KM, Moon EJ, Dhup S, Danhier P, Frérart F, Gallez B, Ribeiro A, Michiels C, Dewhirst MW and Feron O. (2012). “Targeting the Lactate Transporter MCT1 in Endothelial Cells Inhibits Lactate-Induced HIF-1 Activation and Tumor Angiogenesis.” *PLOS ONE* 7: e33418.

Takada Y, Mukhopadhyay A, Kundu GC, Mahabeleshwar GH, Singh S and Aggarwal BB. (2003). “Hydrogen Peroxide Activates NF-Kappa B through Tyrosine Phosphorylation of I Kappa B Alpha and Serine Phosphorylation of P65: Evidence for the Involvement of I Kappa B Alpha Kinase and Syk Protein-Tyrosine Kinase.” *The Journal of Biological Chemistry* 278: 24233–24241.

Takeuchi O and Akira S. (2010). “Pattern Recognition Receptors and Inflammation.” *Cell* 140: 805–820.

Tan Z, Xie N, Cui H, Moellering DR, Abraham E, Thannickal VJ and Liu G. (2015). “Pyruvate Dehydrogenase Kinase 1 Participates in Macrophage Polarization via Regulating Glucose Metabolism.” *The Journal of Immunology* 194: 6082–6089.

Tannahill GM, Curtis AM, Adamik J, Palsson-Mcdermott EM, McGettrick AF, Goel G, Frezza C, Bernard NJ, Kelly B, Foley NH, Zheng L, Gardet A, Tong Z, Jany SS, Corr SC, Haneklaus M, Caffrey BE, Pierce K, Walmsley S, Beasley FC, Cummins E, Nizet V, Whyte M, Taylor CT, Lin H, Masters SL, Gottlieb E, Kelly VP, Clish C, Auron PE, Xavier RJ and O’Neill LAJ. (2013). “Succinate Is an Inflammatory Signal That Induces IL-1β through HIF-1α.” *Nature* 496: 238–242.

Varol C, Mildner A and Jung S. (2015). “Macrophages: Development and Tissue Specialization.” *Annual Review of Immunology* 33: 643–675.

Verma A, Kroetz DN, Tweedle JL and Deepe GS. (2015). “Type II Cytokines Impair Host Defense against an Intracellular Fungal Pathogen by Amplifying Macrophage Generation of IL-33.” *Mucosal Immunology* 8: 380–389.

Vignesh KS, Landero Figueroa JA, Porollo A, Caruso JA and Deepe GS. (2013). “Granulocyte Macrophage-Colony Stimulating Factor-Induced Zn Sequestration Enhances Macrophage Superoxide and Limits Intracellular Pathogen Survival.” *Immunity* 39: 697–710.

Warburg O. (1925). “Über Den Stoffwechsel Der Carcinomzelle.” *Klinische Wochenschrift* 4: 534–536.

Weidemann A and Johnson RS. (2008). “Biology of HIF-1alpha.” *Cell Death and Differentiation* 15: 621–627.

Werth N, Beerlage C, Rosenberger C, Yazdi AS, Edelmann M, Amr A, Bernhardt W, Eiff C von, Becker K, Schäfer A, Peschel A and Kempf VAJ. (2010). “Activation of Hypoxia Inducible Factor 1 Is a General Phenomenon in Infections with Human Pathogens.” *PLOS ONE* 5: e11576.

West AP, Brodsky IE, Rahner C, Woo DK, Erdjument-Bromage H, Tempst P, Walsh MC, Choi Y, Shadel GS and Ghosh S. (2011). “TLR Signalling Augments Macrophage Bactericidal Activity through Mitochondrial ROS.” *Nature* 472: 476–480.

Winters MS, Chan Q, Caruso JA and Deepe, Jr GS. (2010). “Metallomic Analysis of Macrophages Infected with *Histoplasma Capsulatum* Reveals a Fundamental Role for Zinc in Host Defenses.” *The Journal of Infectious Diseases* 202: 1136–1145.

Woods JP. (2016). “Revisiting Old Friends: Developments in Understanding *Histoplasma Capsulatum* Pathogenesis.” *Journal of Microbiology* 54: 265–276.

Wu-Hsieh BA, Lee GS, Franco M and Hofman FM. (1992). “Early Activation of Splenic Macrophages by Tumor Necrosis Factor Alpha Is Important in Determining the Outcome of Experimental Histoplasmosis in Mice.” *Infection and Immunity* 60: 4230–4238.

Wyatt E V, Diaz K, Griffin AJ, Rasmussen JA, Crane DD, Jones BD and Bosio CM. (2016). “Metabolic Reprogramming of Host Cells by Virulent *Francisella Tularensis* for Optimal Replication and Modulation of Inflammation.” *The Journal of Immunology* 196: 4227–4236.

Yona S, Kim K-W, Wolf Y, Mildner A, Varol D, Breker M, Strauss-Ayali D, Viukov S, Guilliams M, Misharin A, Hume DA, Perlman H, Malissen B, Zelzer E and Jung S. (2013). “Fate Mapping Reveals Origins and Dynamics of Monocytes and Tissue Macrophages under Homeostasis.” *Immunity* 38: 79–91.

Zhou P, Sieve MC, Bennett J, Kwon-Chung KJ, Tewari RP, Gazzinelli RT, Sher A and Seder RA. (1995). “IL-12 Prevents Mortality in Mice Infected with *Histoplasma Capsulatum* through Induction of IFN-Gamma.” *The Journal of Immunology* 155: 785–795.

Zinkernagel AS, Johnson RS and Nizet V. (2007). “Hypoxia Inducible Factor (HIF) Function in Innate Immunity and Infection.” *Journal of Molecular Medicine* 85: 1339–1346.

6.2 Books and dissertations

Ahmed MA, “Exploring the Impact of Hypoxia Mimetic Agents on Multipotent Stem Cell Biology.” Dissertation from the Faculty of Medicine and Health Sciences, Keele University, 2018

DuBois JC, “The Role of Hypoxic Adaptation in the Pathogenesis of Histoplasmosis.” Dissertation from the College of Medicine, University of Cincinnati, 2015

Friedrich D, “HIF-1α drives fungal immunity in human macrophages” Dissertation from the Department of Natural Sciences, University of Lübeck, 2016

Golenhofen K, „Sauerstoff-Partialdruck und Sauerstoff-Gehalt“ in Golenhofen K: “Schwarze Reihe: Physiologie”, 22. Auflage, 265, Georg Thieme Verlag KG, Stuttgart, 2011

Zech R, “Abbau der Kohlenhydrate” in Zech R: “Schwarze Reihe: Biochemie”, 18. Auflage, 201, Georg Thieme Verlag KG, Stuttgart, 2006

7 Appendix

7.1 Publications

Friedrich D, Zapf D, Lohse B, Fecher R, Deepe G, Rupp J. (2019). “The HIF-1α/LC3-II-axis impacts on fungal immunity in human macrophages” *Infection and Immunity* 87:e00125-19

7.2 Conference Contributions

7.2.1 Talks

Lohse B., Friedrich D., Rupp J. “Interaction of human alveolar macrophages and *Histoplasma capsulatum*” IRTG1911 Retreat 10/2016 in Boltenhagen, Germany

7.2.2 Posters

Lohse B., Deepe GS., Rupp J., “Interaction of human alveolar macrophage and *Histoplasma capsulatum*” IRTG1911 On-Site-Visit 01/2017 in Lübeck, Germany

Lohse B., Friedrich D., Deepe GS., Rupp J. „Der Feind im Inneren: Modell einer Pilzinfektion der Lunge“ Uni im Dialog 06/2017 in Lübeck, Germany

Lohse B., Friedrich D., Zapf D., Deepe GS., Rupp J „*Histoplasma capsulatum* shapes host cell metabolism in alveolar macrophages“ DGHM Congress 02/2018 in Bochum, Germany

7.3 Ethics

All procedures were performed as described and according to the vote of the ethics committee from August 4th, 2016, issued under the file reference 16-198.

8. Acknowledgements

This thesis contains the thoughts and efforts of so many and the very least they deserve is recognition and gratefulness.

Firstly, I would like to thank Prof. Dr. med. Jan Rupp for supervising and hosting my work at his department. His scientific input and discussions greatly supported me for the past years.

I am thankful for the support of Dirk Friedrich and Dorinja Zapf who taught me the entire laboratory how-to. They put up with my problems and ideas no matter how absurd, helped me around the pitfalls, read through and commented presentations, posters and reports.

I want to thank all the other members of the AG Rupp for their comments, ideas and suggestions during our lab meetings.

I appreciated the support from our laboratory technicians Anke Hellberg, Siegrid Pätzmann and Angela Gravenhorst.

Gratitude on a not only scientific level is owed to my fellow MD students Claudia Lanzer, Jonathan Olbertz, Tobias Vanselow and Maximilian Wanker. Thank you for sharing your experiences, making coffee and cracking jokes.

I very much thank Prof. George S. Deepe Jr. MD not only for hosting me at his department, but especially for his great expertise in *Histoplasma capsulatum* research, which he never is and never will be tired to share with anyone who wants to hear it.

I also want to thank all the members of the Deepe lab for welcoming me to their work group. Special credits go to Bill Buesing who ever joyfully helped me around the lab and gladly collected alveolar MΦ with me at the end of the day.

For providing BAL fluid, I want to thank Dr. med. Daniel Drömann and his team at the Medical Department III and especially Ute Knuppertz for the great coordination. For helping me with the electron microscopic pictures I want thank Prof. Dr. med. Matthias Klinger.

Further, I am thankful for scientific and financial support from the IRTG 1911 headed by Prof. Dr. med Jörg Köhl.

Finally, I want to express my gratitude towards my friends and family, who supported me all the way. You encouraged me when I failed, you cheered with me when I succeeded, you kept me going when I didn't want to. Thank you.

9. Curriculum vitae

Björn Lohse

born 1994

Education

University

Medical student at University of Lübeck, Germany (October 2012 – ongoing)

1st state examination August 2014 (Grade 1,0)

2nd state examination April 2019 (Grade 1,0)

ERASMUS exchange student at University of Ljubljana, Slovenia

(September 2018 – January 2019)

Basic education

Lloydgymnasium Bremerhaven, Germany (2004 - 2012)

Altwulsdorfer Schule Bremerhaven, Germany (2000-2004)

Scientific research

MD researcher

University of Lübeck, Department of Infectious Diseases and Microbiology, research group of Prof. Dr. med. Jan Rupp

Experimental period (October 2016 – September 2017)

Doctoral thesis “Der Einfluss von HIF-1α und metabolischen Interaktionen auf *Histoplasma capsulatum* Infektionen in Alveolarmakrophagen“ (concluded 2020)

University of Cincinnati College of Medicine, Division of Infectious Diseases, research group of Prof. George S. Deepe Jr. MD (January 2017 – April 2017)

Scholarships

Scholar of “Studienstiftung des deutschen Volkes” since 2015

MD scholar of the IRTG 1911 Project B8 (October 2016 – September 2017)